human hepatoma cells. We demonstrated the activation of 2′5′-OAS and IFN-stimulated response element (ISRE) by IFN-α using the reporter assay system in our HuH-7-derived OR6 cells. However, we could not obtain evidence that teprenone activated both 2′5′-OAS and ISRE promoters (supporting information, Fig. S2A and B). Signal transducer and activator of transcription (STAT)1 and STAT2 were not phosphorylated after treatment with teprenone (supporting information, Fig. S2C). This discrepancy may have been caused by the heterogeneity of HuH-7 cells, because OR6 was selected as the clonal cell line and is highly susceptible to HCV RNA replication. Further study is needed to clarify the mechanism underlying teprenone's effect on IFN signalling.

Teprenone reportedly protects the gastric mucosa by inducing HSP (24). From this standpoint, the anti-HCV activity of teprenone was an unexpected result, because recently, it was reported that HSP90 is essential for HCV RNA replication and that an HSP90 inhibitor, geldanamycin, inhibits HCV RNA replication (25, 26). We examined whether or not teprenone induced HSP90 in hepatoma cells and found that it did not (supporting information, Fig. S4).

In this study, we monitored the geranylgeranylated state of Rap1A as a marker using nongeranylgeranylated Rap1A-detectable anti-Rap1A antibody (sc-1482). The least expected result of this sensitive geranylgeranylation assay is that teprenone enhanced statins' inhibitory action against geranylgeranylation. It is not clear in this study as to why teprenone enhanced statins' inhibitory action on geranylgeranylation. One possibility is that teprenone may cause biosynthesis from FPP to cholesterol rather than to GGPP by an unknown mechanism. To clarify this point, further study will be needed. This new function of teprenone may contribute to not only the antiviral field but also other fields, including studies on osteoporosis and on various kinds of antitumours, because geranylgeranylation and farnesylation are targets of the reagent in these fields. For example, statins interfere with the production of GGPP and FPP, which is important in the activation of small G proteins, such as K-ras and the Rho family, and disrupt the growth of malignant cells.

Recently, two important findings have been reported. Firstly, El-Serag *et al.* (8) reported that statins are associated with a reduced risk of HCC. Secondly, Abraldes *et al.* (9) reported that statin lowers portal pressure in patients with cirrhosis. Therefore, as teprenone is a strong adjuvant to statin's inhibitory action against geranylgeranylation, it may further improve portal hypertension in cirrhosis and reduce the risk of HCC in combination with statins. Although teprenone alone possesses modest anti-HCV activity, it will play a significant role in combination with IFN and/or statins in the therapy to HCV-associated liver diseases as an adjuvant like ribavirin. As teprenone is available in clinical use with a low side effect, a clinical study using teprenone in combination with IFN-α and/or statins is now underway in our institution.

In conclusion, we have shown that the anti-ulcer agent teprenone inhibited HCV RNA replication and enhanced statins' inhibitory action against geranylgeranylation. This newly discovered function of teprenone may contribute to improve the treatment of HCV-associated liver diseases (CH C, cirrhosis and HCC) as an adjuvant to statins.

Acknowledgements

The authors would like to thank Atsumi Morishita, Takashi Nakamura and Midori Takeda for their technical assistance. This work was supported by grants-in-aid for a third-term comprehensive 10-year strategy for cancer control and for research on hepatitis from the Ministry of Health, Labor, and Welfare of Japan. K. A. and K. M. were supported by a Research Fellowship from the Japan Society for the Promotion of Science (JSPS) for Young Scientists.

References

1. Feld JJ, Hoofnagle JH. Mechanism of action of interferon and ribavirin in treatment of hepatitis C. *Nature* 2005; **436**: 967–72.
2. Ikeda M, Abe K, Dansako H, *et al.* Efficient replication of a full-length hepatitis C virus genome, strain O, in cell culture, and development of a luciferase reporter system. *Biochem Biophys Res Commun* 2005; **329**: 1350–9.
3. Ikeda M, Abe K, Yamada M, *et al.* Different anti-HCV profiles of statins and their potential for combination therapy with interferon. *Hepatology* 2006; **44**: 117–25.
4. Ikeda M, Kato N. Modulation of host metabolism as a target of new antivirals. *Adv Drug Deliv Rev* 2007; **59**: 1277–89.
5. Ikeda M, Kato N. Life style-related diseases of the digestive system: cell culture system for the screening of anti-hepatitis C virus HCV reagents: suppression of HCV replication by statins and synergistic action with interferon. *J Pharmacol Sci* 2007; **105**: 145–50.
6. Kim SS, Peng LF, Lin W, *et al.* A cell-based, high-throughput screen for small molecule regulators of hepatitis C virus replication. *Gastroenterology* 2007; **132**: 311–20.
7. Bader T, Fazili J, Madhoun M, *et al.* Fluvastatin inhibits hepatitis C replication in humans. *Am J Gastroenterol* 2008; **103**: 1383–9.
8. El-Serag HB, Johnson ML, Hachem C, Morgana RO. Statins are associated with a reduced risk of hepatocellular carcinoma in a large cohort of patients with diabetes. *Gastroenterology* 2009; **136**: 1601–8.
9. Abraldes JG, Albillos A, Banares R, *et al.* Simvastatin lowers portal pressure in patients with cirrhosis and portal hypertension: a randomized controlled trial. *Gastroenterology* 2009; **136**: 1651–8.

10. Kapadia SB, Chisari FV. Hepatitis C virus RNA replication is regulated by host geranylgeranylation and fatty acids. *Proc Natl Acad Sci USA* 2005; **102**: 2561–6.
11. Ye J, Wang C, Sumpter R Jr, *et al.* Disruption of hepatitis C virus RNA replication through inhibition of host protein geranylgeranylation. *Proc Natl Acad Sci USA* 2003; **100**: 15865–70.
12. Wang C, Gale M Jr, Keller BC, *et al.* Identification of FBL2 as a geranylgeranylated cellular protein required for hepatitis C virus RNA replication. *Mol Cell* 2005; **18**: 425–34.
13. Lindenbach BD, Evans MJ, Syder AJ, *et al.* Complete replication of hepatitis C virus in cell culture. *Science* 2005; **309**: 623–6.
14. Wakita T, Pietschmann T, Kato T, *et al.* Production of infectious hepatitis C virus in tissue culture from a cloned viral genome. *Nat Med* 2005; **11**: 791–6.
15. Zhong J, Gastaminza P, Cheng G, *et al.* Robust hepatitis C virus infection in vitro. *Proc Natl Acad Sci USA* 2005; **102**: 9294–9.
16. Nanke Y, Kotake S, Ninomiya T, *et al.* Geranylgeranylacetone inhibits formation and function of human osteoclasts and prevents bone loss in tail-suspended rats and ovariectomized rats. *Calcif Tissue Int* 2005; **77**: 376–85.
17. Kato N, Sugiyama K, Namba K, *et al.* Establishment of a hepatitis C virus subgenomic replicon derived from human hepatocytes infected in vitro. *Biochem Biophys Res Commun* 2003; **306**: 756–66.
18. Naka K, Ikeda M, Abe K, Dansako H, Kato N. Mizoribine inhibits hepatitis C virus RNA replication: effect of combination with interferon-alpha. *Biochem Biophys Res Commun* 2005; **330**: 871–9.
19. Dansako H, Naganuma A, Nakamura T, *et al.* Differential activation of interferon-inducible genes by hepatitis C virus core protein mediated by the interferon stimulated response element. *Virus Res* 2003; **97**: 17–30.
20. Ariumi Y, Kuroki M, Abe K, *et al.* DDX3 DEAD-box RNA helicase is required for hepatitis C virus RNA replication. *J Virol* 2007; **81**: 13922–6.
21. Hughes A, Rogers MJ, Idris AI, Crockett JC. A comparison between the effects of hydrophobic and hydrophilic statins on osteoclast function in vitro and ovariectomy-induced bone loss in vivo. *Calcif Tissue Int* 2007; **81**: 403–1.
22. Merrell MA, Wakchoure S, Lehenkari PP, Harris KW, Selander KS. Inhibition of the mevalonate pathway and activation of p38 MAP kinase are independently regulated by nitrogen-containing bisphosphonates in breast cancer cells. *Eur J Pharmacol* 2007; **570**: 27–37.
23. Ichikawa T, Nakao K, Nakata K, *et al.* Geranylgeranylacetone induces antiviral gene expression in human hepatoma cells. *Biochem Biophys Res Commun* 2001; **280**: 933–9.
24. Hirakawa T, Rokutan K, Nikawa T, Kishi K. Geranylgeranylacetone induces heat shock proteins in cultured guinea pig gastric mucosal cells and rat gastric mucosa. *Gastroenterology* 1996; **111**: 345–57.
25. Nakagawa S, Umehara T, Matsuda C, *et al.* Hsp90 inhibitors suppress HCV replication in replicon cells and humanized liver mice. *Biochem Biophys Res Commun* 2007; **353**: 882–8.
26. Okamoto T, Nishimura Y, Ichimura T, *et al.* Hepatitis C virus RNA replication is regulated by FKBP8 and Hsp90. *Embo J* 2006; **25**: 5015–25.

Supporting information

Additional supporting information may be found in the online version of this article:

Fig. S1. The effects of anti-ulcer agents on HCV RNA replication. (A) Cell proliferation assay. OR6 cells were treated with teprenone (0, 2.5, 5, 10, and 20 μg/ml), and the cells at 24, 48, and 72 hours after treatment were subjected to WST-1 cell proliferation assay. (B) Structures of ant-ulcer agents. (C-E) OR6 cells were treated with ecabet sodium (0, 2.5, 5, 10, 20 μg/ml) (C), sofalcon (0, 2.5, 5, 10, 20 μg/ml) (D), and gefarnate (0, 2.5, 5, 10, 20 μg/ml) (E) for 72 hours. Then the cells were subjected to luciferase assay (upper panel) and Western blot analysis using anti-core, and anti-β-actin antibodies (lower panel) as shown in Figure 1B.

Fig. S2. Teprenone didn't activate IFN signaling pathway. (A and B) Luciferase assays for 2'5'OAS and ISRE promoters. p2'5'OAS-luc (A) and pISRE-luc (B) transfected OR6c cells were treated with teprenone (0, 2.5, 5, and 10 μg/ml) or IFN-α (0, 2.5, 5, and 10 IU/ml) for 6 hours and then subjected to luciferase reporter assay. (C) Teprenone didn't activate STATs in OR6 cells. OR6 cells were treated with IFN-α (500 IU/ml), PTV (1.25 μM), and teprenone (20 μg/ml) for 0, 3, 6, and 12 hours. Then the cells were subjected to Western blot analysis using anti-pSTAT1 (Tyr701), anti-STAT1, anti-pSTAT2 (Tyr689), anti-core, and anti-β-actin antibodies.

Fig. S3. Teprenone treatment didn't cause positive feedback of HMG-CoA reductase (HMGCR). OR6c cells were treated with teprenone (20 μg/ml), PTV (10 μmol/L), or neither for 24 hours. The cells were subjected to RT-PCR (A) and real-time RT-quantitative PCR (B) using HMG-CoA reductase-specific primer set. H_2O was used as a negative control. GAPDH was used as an internal control.

Fig. S4. Teprenone didn't induce HSP90 or HSP70 in HuH-7 cells. OR6 cells were treated with teprenone (20 μg/ml) for 0, 3, 6, 12, 24, and 48 hours. Then the cells were subjected to Western blot analysis using anti-HSP90, anti-HSP70 anti-core, and anti-β-actin antibodies.

Please note: Wiley-Blackwell is not responsible for the content or functionality of any supporting materials supplied by the authors. Any queries (other than missing material) should be directed to the corresponding author for the article.

JOURNAL OF VIROLOGY, July 2011, p. 6882–6892 Vol. 85, No. 14
0022-538X/11/$12.00 doi:10.1128/JVI.02418-10

Hepatitis C Virus Hijacks P-Body and Stress Granule Components around Lipid Droplets▽

Yasuo Ariumi,[1,2]* Misao Kuroki,[1] Yukihiro Kushima,[3] Kanae Osugi,[4] Makoto Hijikata,[3] Masatoshi Maki,[4] Masanori Ikeda,[1] and Nobuyuki Kato[1]

Department of Tumor Virology, Okayama University Graduate School of Medicine, Dentistry, and Pharmaceutical Sciences, Okayama 700-8558, Japan[1]; Center for AIDS Research, Kumamoto University, Kumamoto 860-0811, Japan[2]; Department of Viral Oncology, Institute for Virus Research, Kyoto University, Kyoto 606-8507, Japan[3]; and Department of Applied Molecular Biosciences, Graduate School of Bioagricultural Sciences, Nagoya University, Nagoya 464-8601, Japan[4]

Received 19 November 2010/Accepted 21 April 2011

The microRNA miR-122 and DDX6/Rck/p54, a microRNA effector, have been implicated in hepatitis C virus (HCV) replication. In this study, we demonstrated for the first time that HCV-JFH1 infection disrupted processing (P)-body formation of the microRNA effectors DDX6, Lsm1, Xrn1, PATL1, and Ago2, but not the decapping enzyme DCP2, and dynamically redistributed these microRNA effectors to the HCV production factory around lipid droplets in HuH-7-derived RSc cells. Notably, HCV-JFH1 infection also redistributed the stress granule components GTPase-activating protein (SH3 domain)-binding protein 1 (G3BP1), ataxin-2 (ATX2), and poly(A)-binding protein 1 (PABP1) to the HCV production factory. In this regard, we found that the P-body formation of DDX6 began to be disrupted at 36 h postinfection. Consistently, G3BP1 transiently formed stress granules at 36 h postinfection. We then observed the ringlike formation of DDX6 or G3BP1 and colocalization with HCV core after 48 h postinfection, suggesting that the disruption of P-body formation and the hijacking of P-body and stress granule components occur at a late step of HCV infection. Furthermore, HCV infection could suppress stress granule formation in response to heat shock or treatment with arsenite. Importantly, we demonstrate that the accumulation of HCV RNA was significantly suppressed in DDX6, Lsm1, ATX2, and PABP1 knockdown cells after the inoculation of HCV-JFH1, suggesting that the P-body and the stress granule components are required for the HCV life cycle. Altogether, HCV seems to hijack the P-body and the stress granule components for HCV replication.

Hepatitis C virus (HCV) is the causative agent of chronic hepatitis, which progresses to liver cirrhosis and hepatocellular carcinoma. HCV is an enveloped virus with a positive single-stranded 9.6-kb RNA genome, which encodes a large polyprotein precursor of approximately 3,000 amino acid (aa) residues. This polyprotein is cleaved by a combination of the host and viral proteases into at least 10 proteins in the following order: core, envelope 1 (E1), E2, p7, nonstructural 2 (NS2), NS3, NS4A, NS4B, NS5A, and NS5B (12, 13, 21). The HCV core protein, a nucleocapsid, is targeted to lipid droplets (LDs), and the dimerization of the core protein by a disulfide bond is essential for the production of infectious virus (24). Recently, LDs have been found to be involved in an important cytoplasmic organelle for HCV production (26). Budding is an essential step in the life cycle of enveloped viruses. The endosomal sorting complex required for transport (ESCRT) system has been involved in such enveloped virus budding machineries, including that of HCV (5).

DEAD-box RNA helicases with ATP-dependent RNA-unwinding activities have been implicated in various RNA metabolic processes, including transcription, translation, RNA splicing, RNA transport, and RNA degradation (32). Previously, DDX3 was identified as an HCV core-interacting protein by yeast two-hybrid screening (25, 29, 43). Indeed, DDX3 is required for HCV RNA replication (3, 31). DDX6 (Rck/p54) is also required for HCV replication (16, 33). DDX6 interacts with an initiation factor, eukaryotic initiation factor 4E (eIF-4E), to repress the translational activity of mRNP (38). Furthermore, DDX6 regulates the activity of the decapping enzymes DCP1 and DCP2 and interacts directly with Argonaute-1 (Ago1) and Ago2 in the microRNA (miRNA)-induced silencing complex (miRISC) and is involved in RNA silencing. DDX6 localizes predominantly in the discrete cytoplasmic foci termed the processing (P) body. Thus, the P body seems to be an aggregate of translationally repressed mRNPs associated with the translation repression and mRNA decay machinery.

In addition to the P body, eukaryotic cells contain another type of RNA granule termed the stress granule (SG) (1, 6, 22, 30). SGs are aggregates of untranslating mRNAs in conjunction with a subset of translation initiation factors (eIF4E, eIF3, eIF4A, eIFG, and poly(A)-binding protein [PABP]), the 40S ribosomal subunits, and several RNA-binding proteins, including PABP, T cell intracellular antigen 1 (TIA-1), TIA-1-related protein (TIAR), and GTPase-activating protein (SH3 domain)-binding protein 1 (G3BP1). SGs regulate mRNA translation and decay as well as proteins involved in various aspects of mRNA metabolisms. SGs are cytoplasmic phase-dense structures that occur in eukaryotic cells exposed to various environmental stress, including heat, arsenite, viral infection, oxidative conditions, UV irradiation, and hypoxia. Impor-

* Corresponding author. Mailing address: Center for AIDS Research, Kumamoto University, 2-2-1 Honjo, Kumamoto 860-0811, Japan. Phone and fax: 81 96 373 6834. E-mail: ariumi@kumamoto-u.ac.jp.
▽ Published ahead of print on 4 May 2011.

tantly, several viruses target SGs and stress granule components for viral replication (10, 11, 34, 39). Recent studies suggest that SGs and the P body physically interact and that mRNAs may move between the two compartments (1, 6, 22, 28, 30).

miRNAs are a class of small noncoding RNA molecules ~21 to 22 nucleotides (nt) in length. miRNAs usually interact with 3′-untranslated regions (UTRs) of target mRNAs, leading to the downregulation of mRNA expression. Notably, the liver-specific and abundant miR-122 interacts with the 5′-UTR of the HCV RNA genome and facilitates HCV replication (15, 17, 19, 20, 31). Ago2 is at least required for the efficient miR-122 regulation of HCV RNA accumulation and translation (40). However, the molecular mechanism(s) for how DDX6 and miR-122 as well as DDX3 positively regulate HCV replication is not fully understood. Therefore, we investigated the potential role of P-body and stress granule components in HCV replication.

MATERIALS AND METHODS

Cell culture. 293FT cells were cultured in Dulbecco's modified Eagle's medium (DMEM; Invitrogen, Carlsbad, CA) supplemented with 10% fetal bovine serum (FBS). HuH-7-derived RSc cured cells, in which cell culture-generated HCV-JFH1 (JFH1 strain of genotype 2a) (37) could infect and effectively replicate, were cultured in DMEM with 10% FBS as described previously (3–5, 23).

Plasmid construction. To construct pcDNA3-FLAG-DDX6, a DNA fragment encoding DDX6 was amplified from total RNAs derived from RSc cells by reverse transcription (RT)-PCR using KOD-Plus DNA polymerase (Toyobo) and the following pairs of primers: 5′-CGGGATCCAAGATGAGCACGGCC AGAACAGAGAACCCTGTT-3′ (forward) and 5′-CCGCTCGAGTTAAGGT TTCTCATCTTCTACAGGCTCGCT-3′ (reverse). The obtained DNA fragments were subcloned into either BamHI-XhoI site of the pcDNA3-FLAG vector (2), and the nucleotide sequences were determined by BigDye termination cycle sequencing using an ABI Prism 310 genetic analyzer (Applied Biosystems, Foster City, CA).

RNA interference. The following small interfering RNAs (siRNAs) were used: human ATXN2/ATX2/ataxin-2 (siGENOME SMRT pool M-011772-01-005), human PABP1/PABPC1 (siGENOME SMRT pool M-019598-01-005), human Lsm1 (siGENOME SMRT pool M-005124-01-005), human Xrn1 (siGENOME SMRT pool M-013754-01-005), human G3BP1 (ON-TARGETplus SMRT pool L-012099-00-005), human PATL1 (siGENOME SMRT pool M-015591-00-005), and siGENOME nontargeting siRNA pool 1 (D-001206-13-05) (Dharmacon, Thermo Fisher Scientific, Waltham, MA), as a control. siRNAs (25 nM final concentration) were transiently transfected into RSc cells (3–5, 23) using Oligofectamine (Invitrogen) according to the manufacturer's instructions. Oligonucleotides with the following sense and antisense sequences were used for the cloning of short hairpin RNA (shRNA)-encoding sequences targeted to DDX6 (DDX6i) as well as the control nontargeting shRNA (shCon) in a lentiviral vector: 5′-GATCC CCGGAGGAACTAACTCTGAAGTTCAAGAGACTTCAGAGTTAGTTCCT CCTTTTTGGAAA-3′ (sense) and 5′-AGCTTTTCCAAAAAGGAGGAACTAA CTCTGAAGTCTCTTGAACTTCAGAGTTAGTTCCTCCGGG-3′ (antisense) for DDX6i and 5′-GATCCCCGAATCCAGAGGTAATCTACTTCAAGAGA GTAGATTACCTCTGGATTCTTTTTGGAAA-3′ (sense) and 5′-AGCTTTTC CAAAAAGAATCCAGAGGTAATCTACTCTCTTGAAGTAGATTACCTC TGGATTCGGG-3′ (antisense) for shCon. The oligonucleotides described above were annealed and subcloned into the BglII-HindIII site, downstream from an RNA polymerase III promoter of pSUPER (8), to generate pSUPER-DDX6i and pSUPER-shCon, respectively. To construct pLV-DDX6i and pLV-shCon, the BamHI-SalI fragments of the corresponding pSUPER plasmids were subcloned into the BamHI-SalI site of pRDI292, an HIV-1-derived self-inactivating lentiviral vector containing a puromycin resistance marker allowing for the selection of transduced cells (7). pLV-DDX3i, described previously (3), was used.

Lentiviral vector production. The vesicular stomatitis virus G protein (VSV-G)-pseudotyped HIV-1-based vector system was described previously (27, 44). The lentiviral vector particles were produced by the transient transfection of the second-generation packaging construct pCMV-ΔR8.91 (27, 44), the VSV-G-envelope-expressing plasmid pMDG2, as well as pRDI292 into 293FT cells with FuGene6 reagent (Roche Diagnostics, Mannheim, Germany).

HCV infection experiments. The supernatants were collected from cell culture-generated HCV-JFH1 (37)-infected RSc cells (3–5, 23) at 5 days postinfection and stored at −80°C after filtering through a 0.45-μm filter (Kurabo, Osaka, Japan) until use. For infection experiments with HCV-JFH1, RSc cells (1×10^5 cells/well) were plated onto 6-well plates and cultured for 24 h. We then infected the cells at a multiplicity of infection (MOI) of 1 or 4. The culture supernatants were collected at 24 h postinfection, and the levels of the core protein were determined by an enzyme-linked immunosorbent assay (ELISA) (Mitsubishi Kagaku Bio-Clinical Laboratories, Tokyo, Japan). Total RNA was also isolated from the infected cellular lysates by using an RNeasy minikit (Qiagen, Hilden, Germany) for analysis of intracellular HCV RNA. The infectivity of HCV-JFH1 in the culture supernatants was determined by a focus-forming assay at 48 h postinfection. HCV-JFH1-infected cells were detected by using anti-HCV core (CP-9 and CP-11 mixture).

Quantitative RT-PCR analysis. The quantitative RT-PCR analysis of HCV RNA was performed by real-time LightCycler PCR (Roche) as described previously (3–5, 14, 23). We used the following forward and reverse primer sets for the real-time LightCycler PCR: 5′-ATGAGTCATGTGGCAGTGGA-3′ (forward) and 5′-GCTGGCTGTACTTCCTCCAC-3′ (reverse) for DDX3, 5′-ATG AGCACGGCCAGAACAGA-3′ (forward) and 5′-TTGCTGTGTCTGTGTGC CCC-3′ (reverse) for DDX6, 5′-TGACGGGGTCACCCACACTG-3′ (forward) and 5′-AAGCTGTAGCCGCGCTCGGT-3′ (reverse) for β-actin, and 5′-AGA GCCATAGTGGTCTGCGG-3′ (forward) and 5′-CTTTCGCAACCCAACGC TAC-3′ (reverse) for HCV-JFH1.

Preparation of anti-PATL1 antibody. The anti-PATL1 antiserum was raised in rabbits using the glutathione *S*-transferase (GST)-fused PATL1 Ct (C-terminal region of PATL1, aa 450 to 770) as an antigen, and immunoglobulins were affinity purified by using the maltose-binding protein (MBP)-fused PATL1 Ct that was immobilized on an *N*-hydroxysuccinimide (NHS) column (GE Healthcare Bio-Sciences AB, Uppsala, Sweden).

Preparation of LDs. Lipid droplets (LDs) were prepared as described previously (26). Cells were pelleted by centrifugation at 1,500 rpm. The pellet was resuspended in hypotonic buffer (50 mM HEPES [pH 7.4], 1 mM EDTA, 2 mM $MgCl_2$) supplemented with a protease inhibitor cocktail (Nacalai Tesque, Kyoto, Japan) and was incubated for 10 min at 4°C. The suspension was homogenized with 30 strokes of a glass Dounce homogenizer using a tight-fitting pestle (Wheaton, Millville, NJ). A 1/10 volume of 10× isotonic buffer {0.2 M HEPES (pH 7.4), 1.2 M potassium acetate (KoAc), 40 mM magnesium acetate [$Mg(oAc)_2$], and 50 mM dithiothreitol (DTT)} was added to the homogenate. The nuclei were removed by centrifugation at 2,000 rpm for 10 min at 4°C. The supernatant was collected and centrifuged at 16,000 × *g* for 10 min at 4°C. The supernatant was mixed with an equal volume of 1.04 M sucrose in isotonic buffer (50 mM HEPES, 100 mM KCl, 2 mM $MgCl_2$, and protease inhibitor cocktail). The solution was set in a 13.2-ml Polyallomer centrifuge tube (Beckman Coulter, Brea, CA). One milliliter of isotonic buffer was loaded onto the sucrose mixture. The tube was centrifuged at 100,000 × *g* in an SW41Ti rotor (Beckman Coulter) for 1 h at 4°C. After the centrifugation, the LD fraction on the top of the gradient solution was recovered in phosphate-buffered saline (PBS). The collected LD fraction was used for Western blot analysis.

Western blot analysis. Cells were lysed in a buffer containing 50 mM Tris-HCl (pH 8.0), 150 mM NaCl, 4 mM EDTA, 1% Nonidet P-40, 0.1% sodium dodecyl sulfate (SDS), 1 mM DTT, and 1 mM phenylmethylsulfonyl fluoride. Supernatants from these lysates were subjected to SDS-polyacrylamide gel electrophoresis, followed by immunoblot analysis using anti-DDX3 (catalog no. 54257 [NT] and 5428 [IN]; Anaspec, San Jose, CA), anti-DDX6 (A300-460A; Bethyl Laboratories, Montgomery, TX), anti-adipose differentiation-related protein (ADFP; GTX110204; GeneTex, San Antonio, TX), anti-calnexin (NT; Stressgen, Ann Arbor, MI), anti-HCV core (CP-9 and CP-11; Institute of Immunology, Tokyo, Japan), anti-β-actin antibody (A5441; Sigma, St. Louis, MO), anti-ATX2/SCA2 antibody (A302-033A; Bethyl), anti-PABP (sc-32318 [10E10]; Santa Cruz Biotechnology, Santa Cruz, CA), anti-PABP (ab21060; Abcam, Cambridge, United Kingdom), anti-G3BP1 (611126; BD Transduction Laboratories, San Jose, CA), anti-LSM1 (LS-C97364, Life Span Biosciences, Seattle, WA), anti-HSP70 (610607; BD), anti-XRN1 (A300-443A; Bethyl), or anti-PATL1 antibody.

Immunofluorescence and confocal microscopic analysis. Cells were fixed in 3.6% formaldehyde in PBS, permeabilized in 0.1% NP-40 in PBS at room temperature, and incubated with anti-DDX3 antibody (54257 [NT] and 5428 [IN]; Anaspec), anti-DDX3X (LS-C64576; Life Span), anti-DDX6 (A300-460A; Bethyl), anti-HCV core (CP-9 and CP-11), anti-ATX2/SCA2 antibody (A302-033A; Bethyl), anti-ataxin-2 (611378; BD), anti-PABP (ab21060; Abcam), anti-G3BP1 (A302-033A; Bethyl), anti-LSM1 (LS-C97364; Life Span), anti-XRN1

(A300-443A; Bethyl), anti-Dcp2 (A302-597A; Bethyl), anti-human Ago2 (011-22033; Wako, Osaka, Japan), or anti-PATL1 antibody at a 1:300 dilution in PBS containing 3% bovine serum albumin (BSA) for 30 min at 37°C. The cells were then stained with fluorescein isothiocyanate (FITC)-conjugated anti-rabbit antibody (Jackson ImmunoResearch, West Grove, PA) at a 1:300 dilution in PBS containing BSA for 30 min at 37°C. Lipid droplets and nuclei were stained with borondipyrromethene (BODIPY) 493/503 (Molecular Probes, Invitrogen) and DAPI (4′,6-diamidino-2-phenylindole), respectively, for 15 min at room temperature. Following extensive washing in PBS, the cells were mounted onto slides using a mounting medium of 90% glycerin–10% PBS with 0.01% *p*-phenylenediamine added to reduce fading. Samples were viewed under a confocal laser scanning microscope (LSM510; Zeiss, Jena, Germany).

Statistical analysis. A statistical comparison of the infectivities of HCV in the culture supernatants between the knockdown cells and the control cells was performed by using the Student *t* test. *P* values of less than 0.05 were considered statistically significant. All error bars indicate standard deviations.

RESULTS

HCV infection hijacks the P-body components. To investigate the potential role of P-body components in the HCV life cycle, we first examined the alteration of the subcellular localization of DDX3 or DDX6 by HCV-JFH1 infection using confocal laser scanning microscopy as previously described (2), since both DDX3 and DDX6 were identified previously as P-body components (6). For this, we used HuH-7-derived RSc cells, in which cell culture-generated HCV-JFH1 (JFH1 strain of genotype 2a) (37) can infect and effectively replicate (3, 4, 23). HCV-JFH1-infected RSc cells at 60 h postinfection were stained with anti-HCV core antibody, anti-DDX3, and/or anti-DDX6. Lipid droplets (LDs) and nuclei were stained with BODIPY 493/503 and DAPI (4′,6-diamidino-2-phenylindole), respectively. Samples were viewed under a confocal laser scanning microscope. Although we observed that endogenous DDX3 localized in faint cytoplasmic foci in uninfected RSc cells, DDX3 relocalized, formed ringlike structures, and colocalized with the HCV core protein in response to HCV-JFH1 infection (Fig. 1A). On the other hand, endogenous DDX6 was localized in the evident cytoplasmic foci termed P bodies in the uninfected cells (Fig. 1A). DDX6 also relocalized, formed ringlike structures, and colocalized with the core protein in response to HCV-JFH1 infection (Fig. 1A). Although we failed to observe that most of the P bodies of DDX6 perfectly colocalized with DDX3 in uninfected RSc cells (Fig. 1B), we observed a few P bodies of DDX6 colocalized with DDX3 in the uninfected cells (Fig. 1B, arrowheads). Intriguingly, we found that endogenous DDX3 colocalized with endogenous DDX6 in HCV-JFH1-infected cells (Fig. 1B). To further confirm this finding, pHA-DDX3 (41) and pcDNA3-FLAG-DDX6 were cotransfected into 293FT cells. Consequently, we observed that hemagglutinin (HA)-DDX3 colocalized with FLAG-DDX6 in 293FT cells coexpressing HA-DDX3 and FLAG-DDX6 (Fig. 1B), suggesting cross talk of DDX3 with DDX6. Recently, LDs have been found to be involved in an important cytoplasmic organelle for HCV production (26). Indeed, both DDX3 and DDX6 were recruited around LDs in response to HCV infection, while these proteins did not colocalize with LDs in uninfected naïve RSc cells (Fig. 1C). Furthermore, both DDX3 and DDX6 accumulated in the LD fraction of the HCV-JFH1-infected RSc cells; however, we could not detect both proteins in the LD fraction from uninfected control cells (Fig. 1D), suggesting that DDX3 and DDX6 are recruited around LDs in response to HCV infection.

These results suggest that HCV-JFH1 infection disrupts P-body formation. Therefore, we further examined whether or not HCV-JFH1 disrupts the P-body formations of other microRNA effectors, including Ago2; the Sm-like protein Lsm1, which is a subunit of heptameric-ring Lsm1-7, involved in decapping; the 5′-to-3′ exonuclease Xrn1; the decapping activator PATL1; and the decapping enzyme DCP2 (6, 21, 30). As expected, HCV-JFH1 disrupted the P-body formations of Ago2, Lsm1, and Xrn1 as well as PATL1 (Fig. 2). Lsm1, Xrn1, or PATL1 relocalized, formed ringlike structures, and colocalized with the HCV core protein in response to HCV-JFH1 infection, whereas they were localized predominantly in P bodies in uninfected RSc cells (Fig. 2). In fact, we observed that DDX6 colocalized with Ago2, a P-body marker (Fig. 2). In contrast, HCV-JFH1 failed to disrupt the P-body formation of DCP2 (Fig. 2). Thus, these results suggest that HCV disrupts P-body formation through the hijacking of P-body components.

HCV hijacks stress granule components. Since Nonhoff et al. recently reported that DDX6 interacted with ataxin-2 (ATX2) (28), we examined the potential cross talk among DDX6, ATX2, and HCV. Although ATX2 and G3BP1, a well-known stress granule component (36), were dispersed in the cytoplasm at 37°C, both proteins formed discrete aggregates termed stress granules and colocalized with each other in response to heat shock at 43°C for 45 min, indicating that ATX2 is also stress granule component (Fig. 3A). We did not observe prominent colocalization between DDX6 and ATX2 at 37°C (Fig. 3B). In contrast, we found that DDX6 was recruited, juxtaposed, and partially colocalized with stress granules of ATX2 in response to heat shock at 43°C for 45 min in the uninfected RSc cells (Fig. 3B). Notably, ATX2 was recruited, formed the ring-like structures, and partially colocalized with DDX6 in response to HCV-JFH1 infection even at 37°C (Fig. 3B). Furthermore, we noticed that ATX2 was recruited around LDs in HCV-JFH1-infected cells at 72 h postinfection, while ATX2 did not colocalize with LDs in uninfected cells (Fig. 3C), suggesting the colocalization of ATX2 with the HCV core protein in infected cells. Indeed, ATX2 colocalized with the HCV core protein in HCV-JFH1-infected RSc cells at 37°C (Fig. 3D). Moreover, HCV-JFH1 infection induced the colocalization of the core protein with other stress granule components, G3BP1 or PABP1 as well as ATX2 (Fig. 4 and 5). To further confirm our findings, we examined the time course of the redistribution of DDX6 and G3BP1 after inoculation with HCV-JFH1. Consequently, we still detected the P-body formation of DDX6 and dispersed G3BP1 in the cytoplasm, and we did not observe a colocalization between the HCV core protein and DDX6 at 12 and 24 h postinfection (Fig. 4). In contrast, we found that the P-body formation of DDX6 began to be disrupted at 36 h postinfection (Fig. 4). Consistently, G3BP1 formed stress granules at 36 h postinfection (Fig. 4). We then noticed a ringlike formation of DDX6 or G3BP1 and colocalization with the HCV core protein after 48 h postinfection (Fig. 4), suggesting that the disruption of P-body formation and the hijacking of P-body and stress granule components occur in a late step of HCV infection.

We then examined whether or not HCV-JFH1 infection

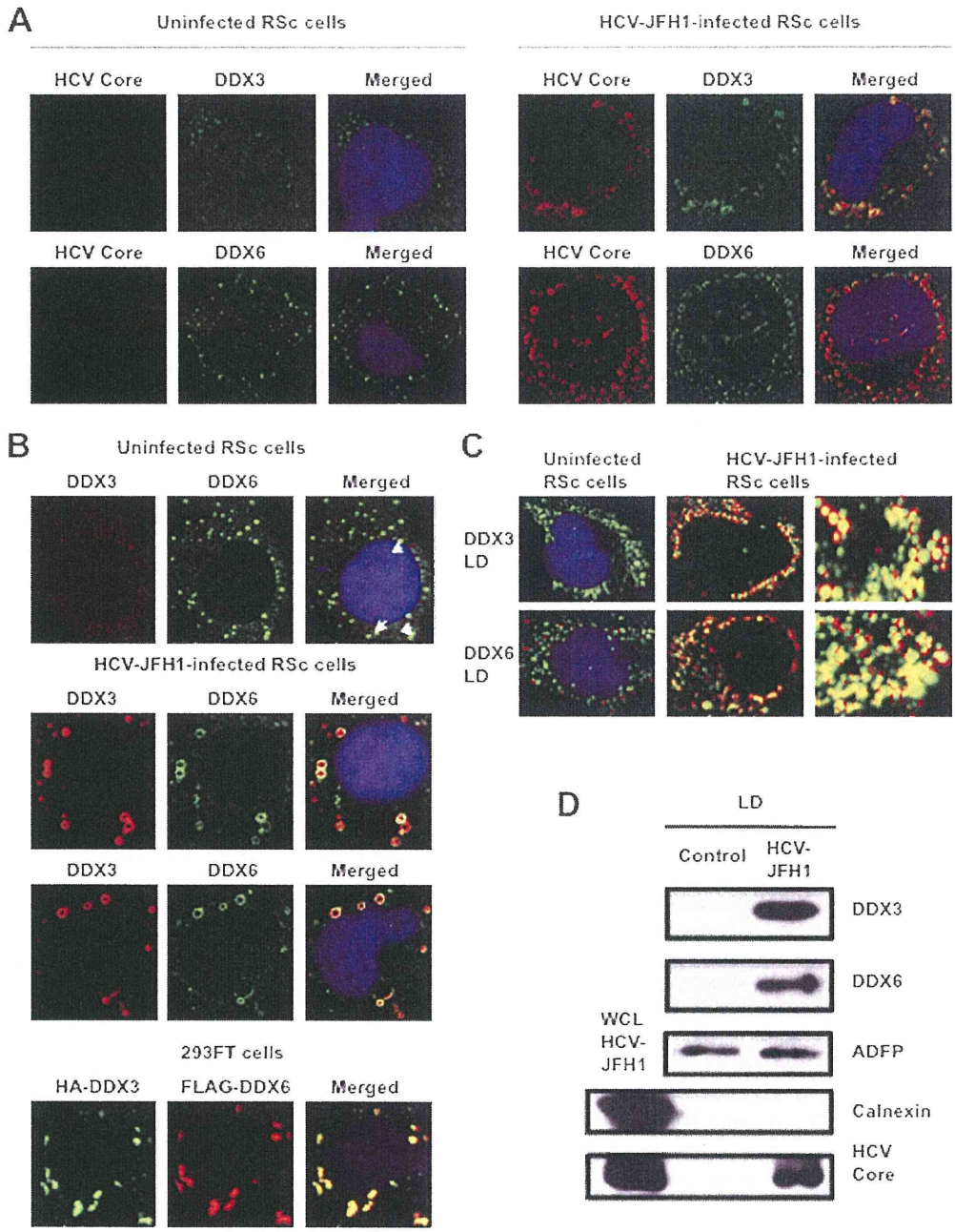

FIG. 1. Dynamic recruitment of DDX3 and DDX6 around lipid droplets (LDs) in response to HCV-JFH1 infection. (A) HCV-JFH1 disrupts the P-body formation of DDX6. Cells were fixed at 60 h postinfection and were then examined by confocal laser scanning microscopy. Cells were stained with anti-HCV core (CP-9 and CP-11 mixture) and either anti-DDX3 (54257 and 54258 mixture) or anti-DDX6 (A300-460A) antibody and then visualized with FITC (DDX3 or DDX6) or Cy3 (core). Images were visualized by using confocal laser scanning microscopy. The two-color overlay images are also exhibited (merged). Colocalization is shown in yellow. (B) HCV-JFH1 recruits DDX3 or DDX6 around LDs. Cells were stained with either anti-DDX3 or anti-DDX6 antibody and were then visualized with Cy3 (red). Lipid droplets and nuclei were stained with BODIPY 493/503 (green) and DAPI (blue), respectively. A high-magnification image is also shown. (C) Colocalization of DDX3 with DDX6. HCV-JFH1-infected RSc cells at 60 h postinfection were stained with anti-DDX3X (LS-C64576) and anti-DDX6 (A300-460A) antibodies. 293FT cells cotransfected with 100 ng of pcDNA3-FLAG-DDX6 and 100 ng of pHA-DDX3 (41) were stained with anti-FLAG-Cy3 and anti-HA-FITC antibodies (Sigma). (D) Association of DDX3 and DDX6 with LDs in response to HCV-JFH1 infection. The LD fraction and whole-cell lysates (WCL) were collected from uninfected RSc cells (control) or HCV-JFH1-infected RSc cells at 5 days postinfection. The results of Western blot analyses of DDX3, DDX6, and the HCV core protein as well as the LD marker ADFP and the endoplasmic reticulum (ER) marker calnexin in the LD fraction are shown.

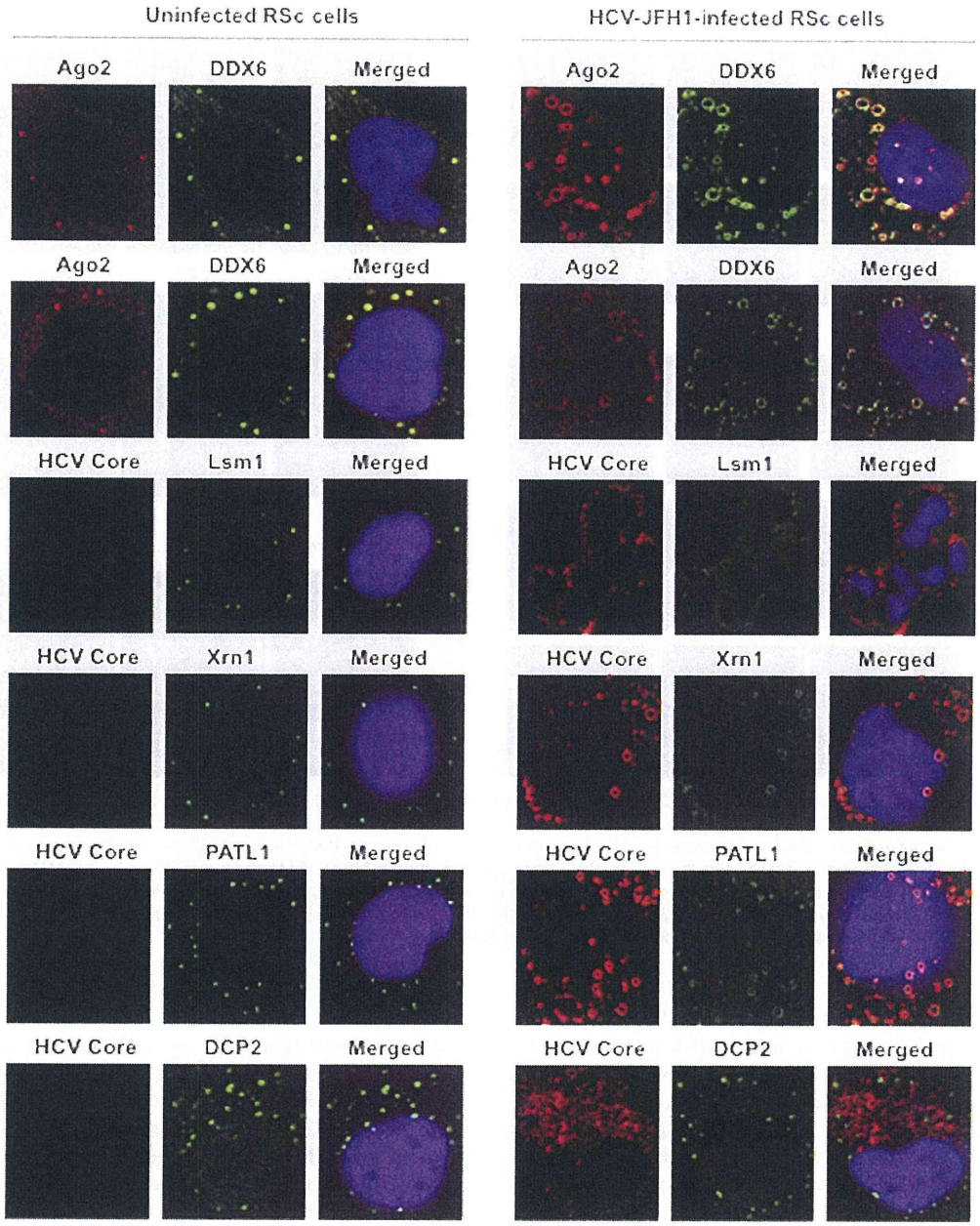

FIG. 2. HCV disrupts the P-body formation of microRNA effectors. Uninfected RSc cells and HCV-JFH1-infected RSc cells at 72 h postinfection were stained with anti-human AGO2 (011-22033) and anti-DDX6 (A300-460A) antibodies. The cells were also stained with anti-HCV core and anti-Lsm1 (LS-C97364), anti-Xrn1 (A300-443A), anti-PATL1, or anti-DCP2 (A302-597A) antibodies and were examined by confocal laser scanning microscopy.

could affect the stress granule formation of G3BP1, ATX2, or PABP1 in response to heat shock or treatment with arsenite. These stress granule components dispersed in the cytoplasm at 37°C, whereas these proteins formed stress granules in response to heat shock at 43°C for 45 min or treatment with 0.5 mM arsenite for 30 min (Fig. 5). In contrast, stress granules were not formed in HCV-JFH1-infected cells at 72 h postinfection in response to heat shock at 43°C for 45 min (Fig. 5), suggesting that HCV-JFH1 infection suppresses stress granule formation in response to heat shock or treatment with arsenite. Intriguingly, G3BP1, ATX2, or PABP1 still colocalized with the HCV core protein even under the above-described stress conditions (Fig. 5). Furthermore, Western blot analysis of cell lysates of uninfected or HCV-JFH1-infected cells at 72 h postinfection showed similar protein expression levels of ATX2, PABP1, HSP70, DDX3, DDX6, and Lsm1 but not G3BP1 (Fig. 6), suggesting that HCV-JFH1 infection does not affect host mRNA translation.

P-body and stress granule components are required for HCV replication. Finally, we investigated the potential role of

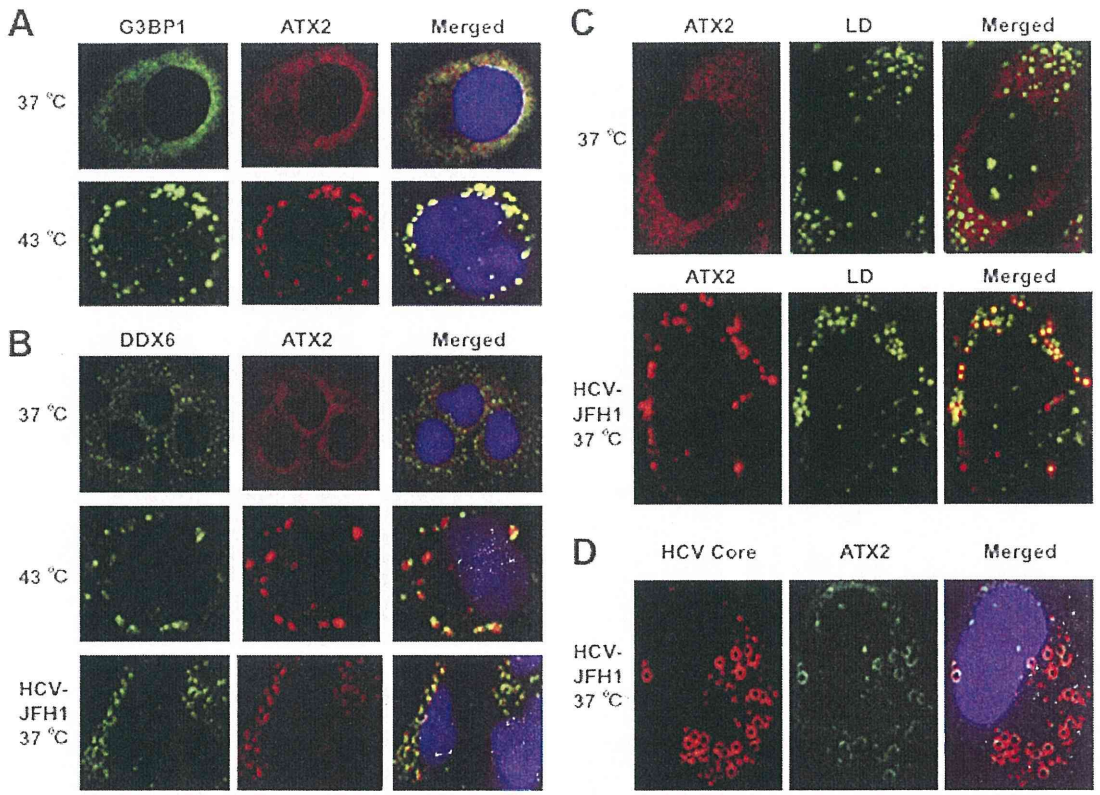

FIG. 3. Dynamic redistribution of ataxin-2 (ATX2) around LDs in response to HCV-JFH1 infection. (A) ATX2 is a stress granule component. RSc cells were incubated at 37°C or 43°C for 45 min. Cells were stained with anti-G3BP1 (A302-033A) and anti-ATX2 (A93520) antibodies and were examined by confocal laser scanning microscopy. (B) Dynamic redistribution of DDX6 and ATX2 in response to heat shock or HCV infection. RSc cells after heat shock at 43°C for 45 min or 72 h after inoculation with HCV-JFH1 were stained with anti-DDX6 and anti-ATX2 (A93520) antibodies. (C) HCV relocalizes ataxin-2 to LDs. HCV-JFH1-infected RSc cells at 72 h postinfection were stained with anti-ATX2 (A93520) antibody and BODIPY 493/503. (D) ATX2 colocalizes with the HCV core protein. HCV-JFH1-infected RSc cells at 72 h postinfection were stained with anti-ATX2/SCA2 (A301-118A) and anti-HCV core antibodies.

P-body and stress granule components in the HCV life cycle. We first used lentiviral vector-mediated RNA interference to stably knock down DDX6 as well as DDX3 in RSc cells. We used puromycin-resistant pooled cells 10 days after lentiviral transduction in all experiments. Real-time LightCycler RT-PCR analysis of DDX3 or DDX6 demonstrated a very effective knockdown of DDX3 or DDX6 in RSc cells transduced with lentiviral vectors expressing the corresponding shRNAs (Fig. 7A). Importantly, shRNAs did not affect cell viabilities (data not shown). We next examined the levels of HCV core and the infectivity of HCV in the culture supernatants as well as the level of intracellular HCV RNA in these knockdown cells 24 h after HCV-JFH1 infection at an MOI of 4. The results showed that the accumulation of HCV RNA was significantly suppressed in DDX3 or DDX6 knockdown cells (Fig. 7B). In this context, the release of the HCV core protein and the infectivity of HCV in the culture supernatants were also significantly suppressed in these knockdown cells (Fig. 7C and D). This finding suggested that DDX6 is required for HCV replication, like DDX3. To further examine the potential role of other P-body and stress granule components in HCV replication, we used RSc cells transiently transfected with a pool of siRNAs specific for ATX2, PABP1, Lsm1, Xrn1, G3BP1, and PATL1 as well as a pool of control siRNAs (siCon) following HCV-JFH1 infection. In spite of the very effective knockdown of each component (Fig. 7E), the siRNAs used in these experiments did not affect cell viabilities (data not shown). Consequently, the accumulation of HCV RNA was significantly suppressed in ATX2, PABP1, or Lsm1 knockdown cells (Fig. 7F), indicting that ATX2, PABP1, and Lsm1 are required for HCV replication. In contrast, the level of HCV RNA was not affected in Xrn1 knockdown cells (Fig. 7F), suggesting that Xrn1 is unrelated to HCV replication. Furthermore, we observed a moderate effect of siG3BP1 and siPATL1 on HCV RNA replication (Fig. 7F). Altogether, HCV seems to hijack the P-body and stress granule components around LDs for HCV replication.

DISCUSSION

So far, the P body and stress granules have been implicated in mRNA translation, RNA silencing, and RNA degradation as well as viral infection (1, 6, 22, 30). Host factors within the P body and stress granules can enhance or limit viral infection, and some viral RNAs and proteins accumulate in the P body and/or stress granules. Indeed, the microRNA effectors DDX6, GW182, Lsm1, and Xrn1 negatively regulate HIV-1 gene expression by preventing the association of viral mRNA

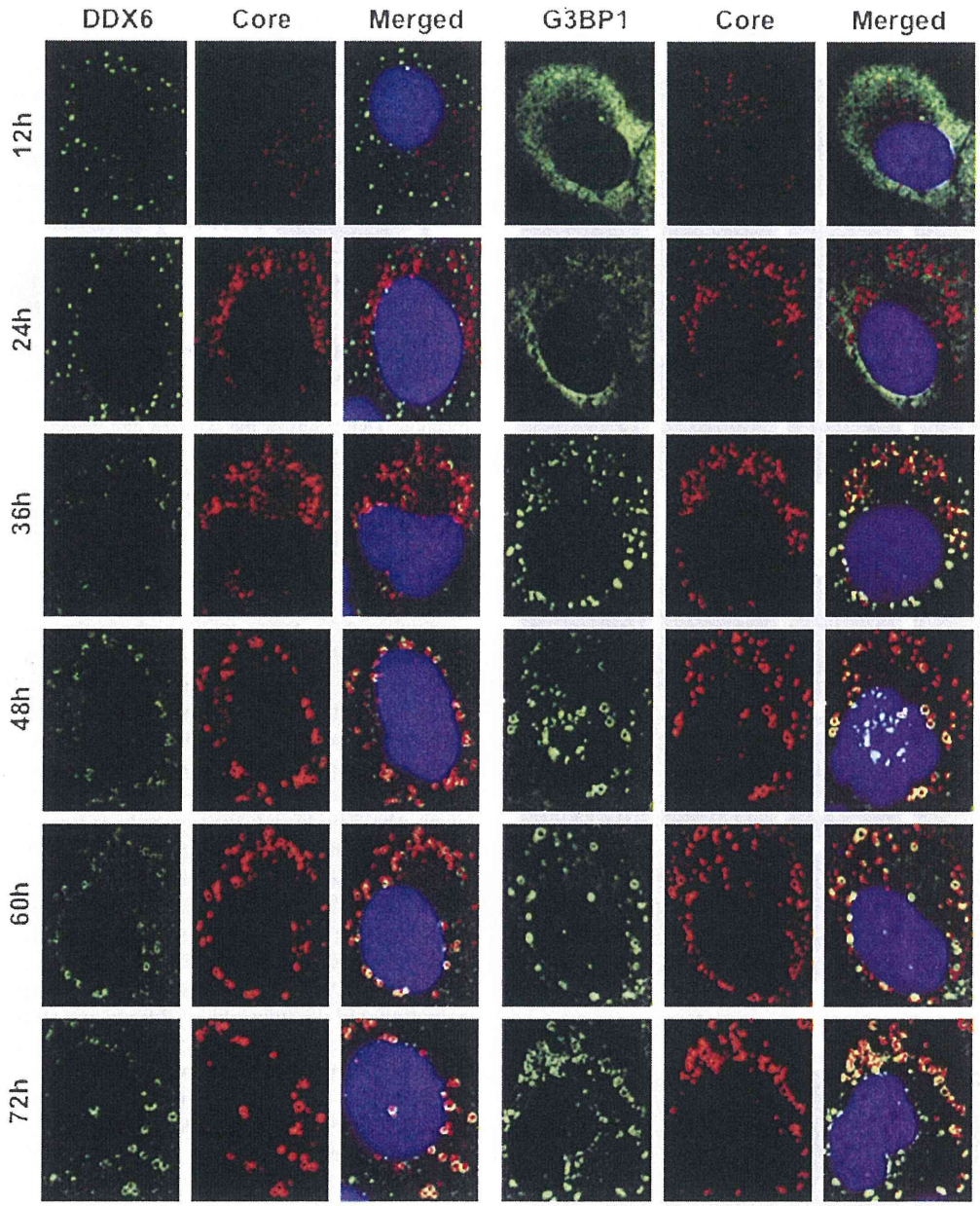

FIG. 4. Dynamic redistribution of DDX6 and G3BP1 in response to HCV-JFH1 infection. RSc cells at the indicated times (hours) after inoculation with HCV-JFH1 were stained with anti-HCV core and either anti-DDX6 (A300-460A) or anti-G3BP1 (A302-033A) antibodies.

with polysomes (9). In contrast, miRNA effectors such as DDX6, Lsm1, PatL1, and Ago2 positively regulate HCV replication (Fig. 7B and F) (16, 31, 33). We have also found that DDX3 and DDX6 are required for HCV RNA replication (3) (Fig. 7B) and that DDX3 colocalized with DDX6 in HCV-JFH1-infected RSc cells (Fig. 1B), suggesting that DDX3 comodulates the DDX6 function in HCV RNA replication. In this regard, the liver-specific miR-122 interacts with the 5′-UTR of the HCV RNA genome and positively regulates HCV replication (15, 17, 19, 20, 31). Since miRNAs usually interact with DDX6 and Ago2 in miRISC and are involved in RNA silencing, DDX6 and Ago2 may be required for miR-122-dependent HCV replication. Indeed, quite recently, a study showed that Ago2 is required for miR-122-dependent HCV RNA replication and translation (40). However, little is known regarding how miR-122 and DDX6 positively regulate HCV replication. Accordingly, we have shown that these miRNA effectors, including DDX6, Lsm1, Xrn1, and Ago2, accumulated around LDs and the HCV production factory and colocalized with the HCV core protein in response to HCV infection (Fig. 1 and 2). However, the decapping enzyme DCP2 did not accumulate and colocalize with the core protein (Fig. 2). Consistent with this finding, Scheller et al. reported previously that the depletion of DCP2 by siRNA did not affect HCV

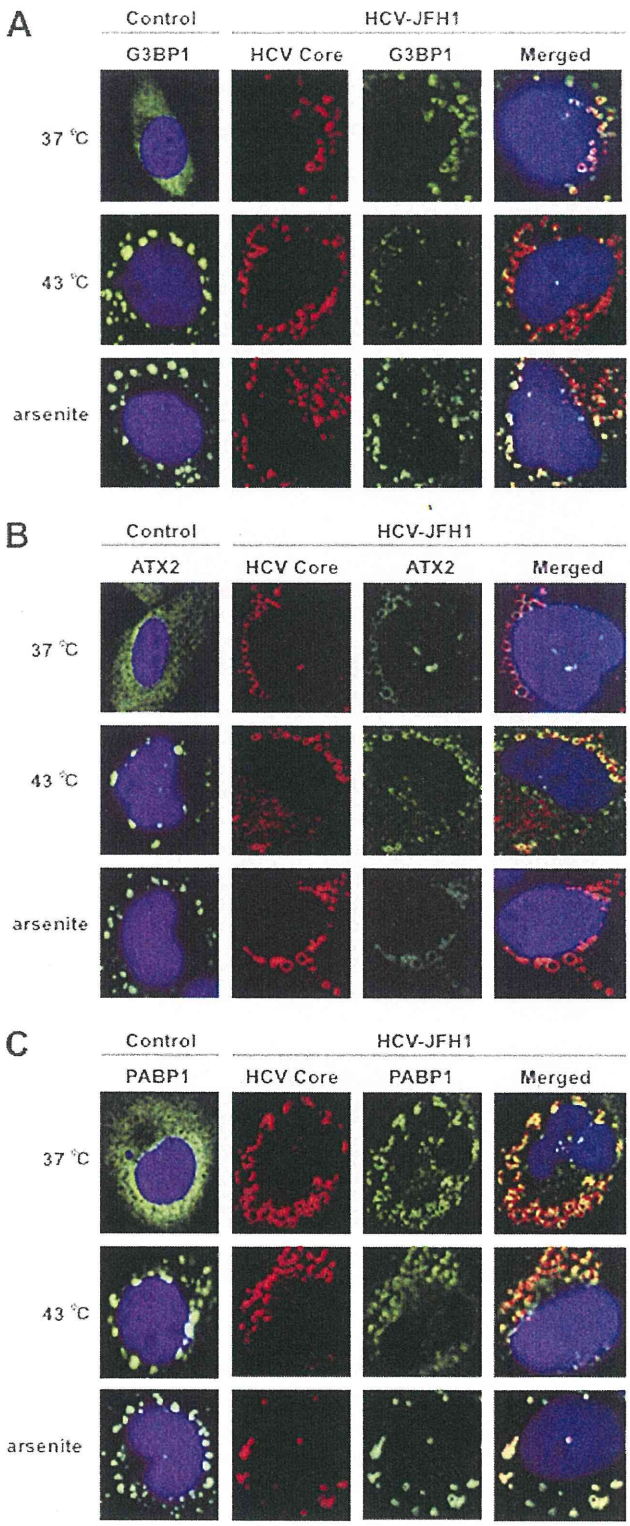

FIG. 5. HCV suppresses stress granule formation in response to heat shock or treatment with arsenite. Naïve RSc cells or HCV-JFH1-infected RSc cells at 72 h postinfection were incubated at 37°C or 43°C for 45 min. Cells were also treated with 0.5 mM arsenite for 30 min. Cells were stained with anti-HCV core and anti-G3BP1 (A), anti-ATX2 (B), or anti-PABP1 (ab21060) (C) antibodies and were examined by confocal laser scanning microscopy.

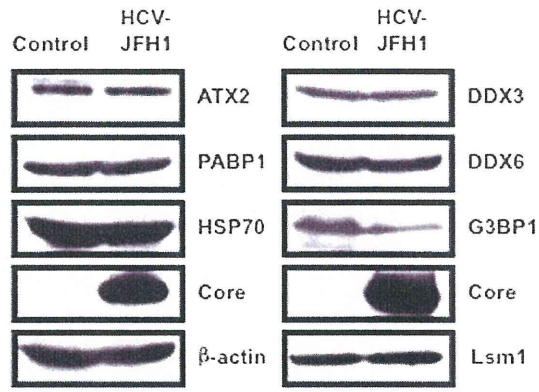

FIG. 6. Host protein expression levels in response to HCV-JFH1 infection. The results of the Western blot analyses of cellular lysates with anti-ATX2/SCA2 antibody (A301-118A), anti-PABP1 (ab21060), anti-HSP70 (610607), anti-HCV core, anti-β-actin, anti-DDX3 (54257 [NT] and 5428 [IN] mixture), anti-DDX6 (A300-460A), anti-G3BP1 (611126), or anti-LSM1 (LS-C97364) antibody in HCV-JFH1-infected RSc cells at 72 h postinfection as well as in naïve RSc cells are shown.

production (33). Since HCV harbors the internal ribosome entry site (IRES) structure in the 5′-UTR of the HCV genome instead of a cap structure, unlike HIV-1, DCP2 may not be recruited on the HCV genome and utilized for HCV replication. Otherwise, DCP2 may determine whether or not DDX6 and miRNAs positively or negatively regulate target mRNA.

Furthermore, we have demonstrated that HCV infection hijacks the P-body and stress granule components around LDs (Fig. 1, 2, 4, and 5). We have found that the P-body formation of DDX6 began to be disrupted at 36 h postinfection (Fig. 4). Consistently, G3BP1 formed stress granules at 36 h postinfection. We then observed the ringlike formation of DDX6 or G3BP1 and colocalization with the HCV core protein after 48 h postinfection, suggesting that the disruption of P-body formation and the hijacking of P-body and stress granule components occur at a late step of HCV infection. Furthermore, HCV infection could suppress stress granule formation in response to heat shock or treatment with arsenite (Fig. 5). In this regard, West Nile virus and dengue virus, of the family *Flaviviridae*, interfere with stress granule formation and P-body assembly through interactions with T cell intracellular antigen 1 (TIA-1)/TIAR (11). Moreover, PABP1 and G3BP1, stress granule components, are known to be common viral targets for the inhibition of host mRNA translation (34, 39). In fact, HIV-1 and poliovirus proteases cleave PABP1 and/or G3BP1 and suppress stress granule formation during viral infection (34, 39). On the other hand, HCV infection transiently induced stress granules at 36 h postinfection (Fig. 4) and did not cleave PABP1 (Fig. 6); however, HCV could suppress stress granule formation in response to heat shock or treatment with arsenite through hijacking their components around LDs, the HCV production factory (Fig. 5). Consistently, Jones et al. showed that HCV transiently induces stress granules of enhanced green fluorescent protein (EGFP)-G3BP at 36 h after infection with the cell culture-generated HCV (HCVcc) reporter virus Jc1FLAG2 (p7-nsGluc2A); however, those authors did not show the recruitment of EGFP-G3BP to LDs (18). Although we do not know the exact reason for this apparent discrepancy,

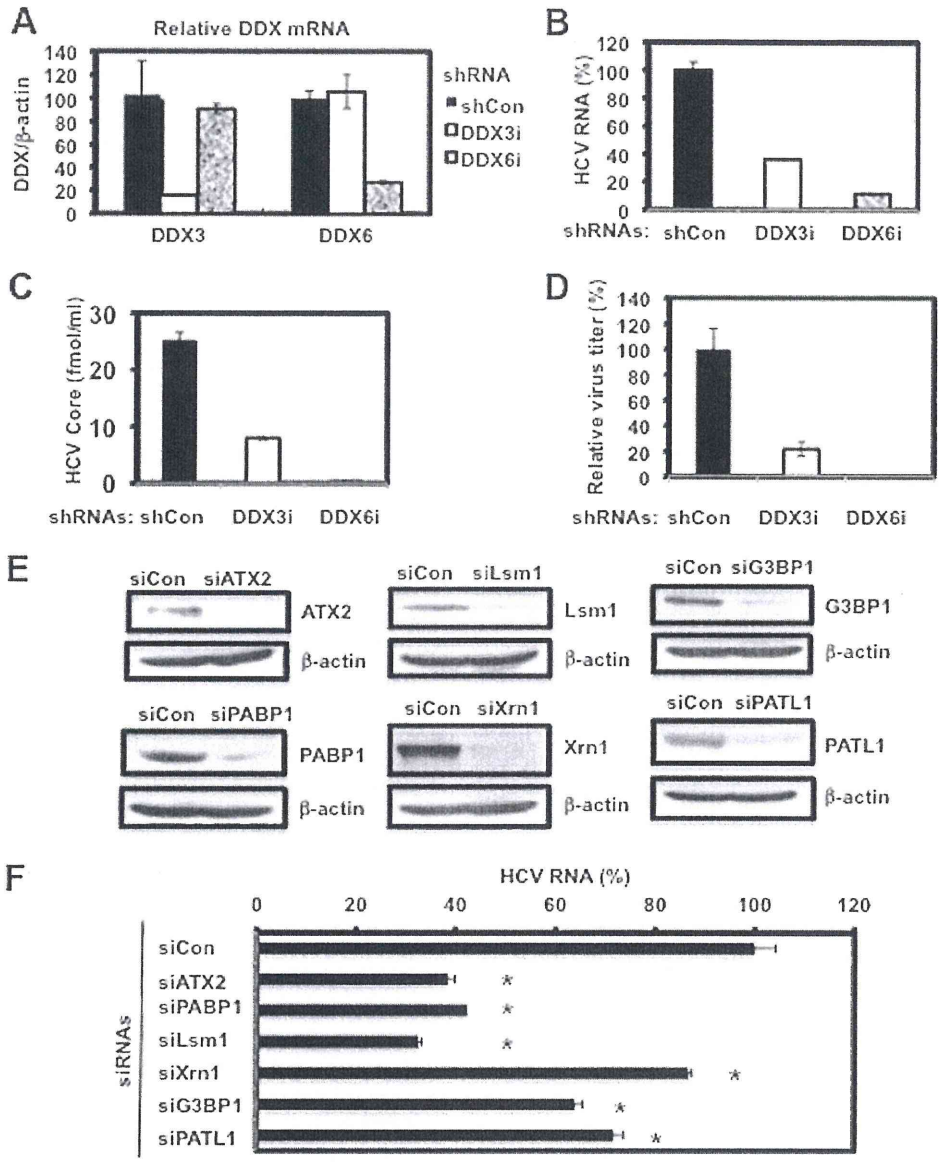

FIG. 7. Requirement of P-body and stress granule components for HCV replication. (A) Inhibition of DDX3 or DDX6 mRNA expression by the shRNA-producing lentiviral vector. Real-time LightCycler RT-PCR for DDX3 or DDX6 was also performed for β-actin mRNA in RSc cells expressing shRNA targeted to DDX3 (DDX3i) or DDX6 (DDX6i) or the control nontargeting shRNA (shCon) in triplicate. Each mRNA level was calculated relative to the level in RSc cells transduced with the control nontargeting lentiviral vector (shCon), which was assigned as 100%. Error bars in this panel and other panels indicate standard deviations. (B) Levels of intracellular genome-length HCV-JFH1 RNA in the cells at 24 h postinfection at an MOI of 4 were monitored by real-time LightCycler RT-PCR. Results from three independent experiments are shown. Each HCV RNA level was calculated relative to the level in RSc cells transduced with a control lentiviral vector (shCon), which was assigned as 100%. (C) The levels of HCV core in the culture supernatants from the stable knockdown RSc cells 24 h after inoculation of HCV-JFH1 at an MOI of 4 were determined by ELISA. Experiments were done in triplicate, and columns represent the mean core protein levels. (D) The infectivity of HCV in the culture supernatants from stable-knockdown RSc cells 24 h after inoculation of HCV-JFH1 at an MOI of 4 was determined by a focus-forming assay at 24 h postinfection. Experiments were done in triplicate, and each virus titer was calculated relative to the level in RSc cells transduced with a control lentiviral vector (shCon), which was assigned as 100%. (E) Inhibition of ATX2, PABP1, Lsm1, Xrn1, G3BP1, or PATL1 protein expression by 72 h after transient transfection of RSc cells with a pool of control nontargeting siRNA (siCon) or a pool of siRNAs specific for ATX2, PABP1, Lsm1, Xrn1, G3BP1, or PATL1 (25 nM), respectively. The results of Western blot analyses of cellular lysates with anti-ATX2, anti-PABP1, anti-Lsm1, anti-Xrn1, anti-G3BP1, anti-PATL1, or anti-β-actin antibody are shown. (F) Levels of intracellular genome-length HCV-JFH1 RNA in the cells at 48 h postinfection at an MOI of 1 were monitored by real-time LightCycler RT-PCR. RSc cells were transiently transfected with a pool of control siRNA (siCon) or a pool of siRNAs specific for ATX2, PABP1, Lsm1, Xrn1, G3BP1, and PATL1 (25 nM). At 48 h after transfection, the cells were inoculated with HCV-JFH1 at an MOI of 1 and incubated for 2 h. The culture medium was then changed and incubated for 22 h. Experiments were done in triplicate, and each HCV RNA level was calculated relative to the level in RSc cells transfected with a control siRNA (siCon), which was assigned as 100%. Asterisks indicate significant differences compared to the control treatment (*, $P < 0.01$).

several possible explanations can be offered. First, those authors examined the localization of EGFP-G3BP within 48 h postinfection, and we observed it at later times (Fig. 4). Second, they used only EGFP-tagged G3BP instead of endogenous G3BP1. Third, they used a Jc1FLAG2 (p7-nsGluc2A) clone, and an HCV-JFH1 clone could markedly induce the recruitment of the core protein to LDs compared to that of Jc1. Also, Jangra et al. failed to observe the recruitment of DDX6 to LDs at 2 days after infection with HJ3-5 virus (16). Accordingly, we also observed that most of the DDX6 still formed intact P bodies at earlier times (12 h or 24 h postinfection). Importantly, we observed the recruitment of DDX6 to LDs 48 h later (Fig. 4). Furthermore, those authors did not show the ringlike structure formation of the HJ3-5 core protein around LDs, unlike the JFH1 core protein that we used in this study. The interaction of the HCV core protein with DDX6 may explain the recruitment of P-body components to LDs. However, we do not yet know whether the P-body function(s) can be performed on LDs. At least, HCV infection did not affect the translation of several host mRNAs with 5′ caps and 3′ poly(A) tails despite the disruption of P-body formation at 72 h postinfection (Fig. 6), suggesting that HCV does not affect P-body function and that HCV recruits functional P bodies to LDs.

We need to address the potential role of stress granule components, such as PABP1, in HCV replication/translation, since the HCV genome does not harbor the 3′ poly(A) tail. Intriguingly, we have found that the accumulation of HCV RNA was significantly suppressed in PABP1 knockdown RSc cells (Fig. 7F). In this regard, Tingting et al. demonstrated previously that G3BP1 and PABP1 as well as DDX1 were identified as the HCV 3′-UTR RNA-binding proteins by proteomic analysis and that G3BP1 was required for HCV RNA replication (35). Yi et al. also reported that G3BP1 was associated with HCV NS5B and that G3BP1 was required for HCV RNA replication (42). We observed a moderate effect of siG3BP1 on HCV RNA replication (Fig. 7F). In contrast, the accumulation of HCV RNA was significantly suppressed in ATX2 and Lsm1 knockdown cells as well as in PABP1 knockdown cells (Fig. 7F), suggesting that ATX2, Lsm1, and PABP1 are required for HCV replication.

Taking these results together, this study has demonstrated for the first time that HCV hijacks P-body and stress granule components around LDs. This hijacking may regulate HCV RNA replication and translation. Indeed, we have found that the accumulation of genome-length HCV-O (genotype 1b) (14) RNA was markedly suppressed in DDX6 knockdown O cells (data not shown). More importantly, these P-body and stress granule components may be involved in the maintenance of the HCV RNA genome without 5′ cap and 3′ poly(A) tail structures in the cytoplasm for long periods, since the hijacking of P-body and stress granule components by HCV occurred at later times.

ACKNOWLEDGMENTS

We thank D. Trono for the lentiviral vector system, T. Wakita for HCV-JFH1, and K. T. Jeang for pHA-DDX3. We also thank T. Nakamura and K. Takeshita for their technical assistance.

This work was supported by a grant-in-aid for scientific research (C) from the Japan Society for the Promotion of Science (JSPS); by a grant-in-aid for research on hepatitis from the Ministry of Health, Labor, and Welfare of Japan; and by the Viral Hepatitis Research Foundation of Japan. M.K. was supported by a research fellowship from the JSPS for young scientists.

REFERENCES

1. **Anderson, P., and N. Kedersha.** 2007. Stress granules: the Tao of RNA triage. Trends Biochem. Sci. **33:**141–150.
2. **Ariumi, Y., et al.** 2003. Distinct nuclear body components, PML and SMRT, regulate the *trans*-acting function of HTLV-1 Tax oncoprotein. Oncogene **22:**1611–1619.
3. **Ariumi, Y., et al.** 2007. DDX3 DEAD-box RNA helicase is required for hepatitis C virus RNA replication. J. Virol. **81:**13922–13926.
4. **Ariumi, Y., et al.** 2008. The DNA damage sensors ataxia-telangiectasia mutated kinase and checkpoint kinase 2 are required for hepatitis C virus RNA replication. J. Virol. **82:**9639–9646.
5. **Ariumi, Y., et al.** 2011. The ESCRT system is required for hepatitis C virus production. PLoS One **6:**e14517.
6. **Beckham, C. J., and R. Parker.** 2008. P bodies, stress granules, and viral life cycles. Cell Host Microbe **3:**206–212.
7. **Bridge, A. J., S. Pebernard, A. Ducraux, A. L. Nicoulaz, and R. Iggo.** 2003. Induction of an interferon response by RNAi vectors in mammalian cells. Nat. Genet. **34:**263–264.
8. **Brummelkamp, T. R., R. Bernard, and R. Agami.** 2002. A system for stable expression of short interfering RNAs in mammalian cells. Science **296:**550–553.
9. **Chable-Bessia, C., et al.** 2009. Suppression of HIV-1 replication by microRNA effectors. Retrovirology **6:**26.
10. **Cristea, I. M., et al.** 2010. Host factors associated with the Sindbis virus RNA-dependent RNA polymerase: role for G3BP1 and G3BP2 in virus replication. J. Virol. **84:**6720–6732.
11. **Emara, M. M., and M. A. Brinton.** 2007. Interaction of TIA-1/TIAR with West Nile and dengue virus products in infected cells interferes with stress granule formation and processing body assembly. Proc. Natl. Acad. Sci. U. S. A. **104:**9041–9046.
12. **Hijikata, M., N. Kato, Y. Ootsuyama, M. Nakagawa, and K. Shimotohno.** 1991. Gene mapping of the putative structural region of the hepatitis C virus genome by in vitro processing analysis. Proc. Natl. Acad. Sci. U. S. A. **88:**5547–5551.
13. **Hijikata, M., et al.** 1993. Proteolytic processing and membrane association of putative nonstructural proteins of hepatitis C virus. Proc. Natl. Acad. Sci. U. S. A. **90:**10773–10777.
14. **Ikeda, M., et al.** 2005. Efficient replication of a full-length hepatitis C virus genome, strain O, in cell culture, and development of a luciferase reporter system. Biochem. Biophys. Res. Commun. **329:**1350–1359.
15. **Jangra, R. K., M. Yi, and S. M. Lemon.** 2010. Regulation of hepatitis C virus translation and infectious virus production by the microRNA miR-122. J. Virol. **84:**6615–6625.
16. **Jangra, R. K., M. Yi, and S. M. Lemon.** 2010. DDX6 (Rck/p54) is required for efficient hepatitis C virus replication but not IRES-directed translation. J. Virol. **84:**6810–6824.
17. **Ji, H., et al.** 2008. MicroRNA-122 stimulates translation of hepatitis C virus RNA. EMBO J. **27:**3300–3310.
18. **Jones, C. T., et al.** 2010. Real-time imaging of hepatitis C virus infection using a fluorescent cell-based reporter system. Nat. Biotechnol. **28:**167–171.
19. **Jopling, C. L., M. Yi, A. M. Lancaster, S. M. Lemon, and P. Sarnow.** 2005. Modulation of hepatitis C virus RNA abundance by a liver-specific microRNA. Science **309:**1577–1581.
20. **Jopling, C. L., S. Schütz, and P. Sarnow.** 2008. Position-dependent function for a tandem microRNA miR-122-binding site located in the hepatitis C virus RNA genome. Cell Host Microbe **4:**77–85.
21. **Kato, N., et al.** 1990. Molecular cloning of the human hepatitis C virus genome from Japanese patients with non-A, non-B hepatitis. Proc. Natl. Acad. Sci. U. S. A. **87:**9524–9528.
22. **Kedersha, N., and P. Anderson.** 2007. Mammalian stress granules and processing bodies. Methods Enzymol. **431:**61–81.
23. **Kuroki, M., et al.** 2009. Arsenic trioxide inhibits hepatitis C virus RNA replication through modulation of the glutathione redox system and oxidative stress. J. Virol. **83:**2338–2348.
24. **Kushima, Y., T. Wakita, and M. Hijikata.** 2010. A disulfide-bonded dimer of the core protein of hepatitis C virus is important for virus-like particle production. J. Virol. **84:**9118–9127.
25. **Mamiya, N., and H. J. Worman.** 1999. Hepatitis C virus core protein binds to a DEAD box RNA helicase. J. Biol. Chem. **274:**15751–15756.
26. **Miyanari, Y., et al.** 2007. The lipid droplet is an important organelle for hepatitis C virus production. Nat. Cell Biol. **9:**1089–1097.
27. **Naldini, L., et al.** 1996. In vivo gene delivery and stable transduction of nondividing cells by a lentiviral vector. Science **272:**263–267.
28. **Nonhoff, U., et al.** 2007. Ataxin-2 interacts with the DEAD/H-box RNA helicase DDX6 and interferes with P-bodies and stress granules. Mol. Biol. Cell **18:**1385–1396.
29. **Owsianka, A. M., and A. H. Patel.** 1999. Hepatitis C virus core protein interacts with a human DEAD box protein DDX3. Virology **257:**330–340.

30. **Parker, R., and U. Sheth.** 2007. P bodies and the control of mRNA translation and degradation. Mol. Cell **25**:635–646.
31. **Randall, G., et al.** 2007. Cellular cofactors affecting hepatitis C virus infection and replication. Proc. Natl. Acad. Sci. U. S. A. **104**:12884–12889.
32. **Rocak, S., and P. Linder.** 2004. DEAD-box proteins: the driving forces behind RNA metabolism. Nat. Rev. Mol. Cell Biol. **5**:232–241.
33. **Scheller, N., et al.** 2009. Translation and replication of hepatitis C virus genomic RNA depends on ancient cellular proteins that control mRNA fates. Proc. Natl. Acad. Sci. U. S. A. **106**:13517–13522.
34. **Smith, R. W., and N. K. Gray.** 2010. Poly(A)-binding protein (PABP): a common viral target. Biochem. J. **426**:1–11.
35. **Tingting, P., F. Caiyun, Y. Zhigang, Y. Pengyuan, and Y. Zhenghong.** 2006. Subproteomic analysis of the cellular proteins associated with the 3′ untranslated region of the hepatitis C virus genome in human liver cells. Biochem. Biophys. Res. Commun. **347**:683–691.
36. **Tourrière, H., et al.** 2003. The RasGAP-associated endoribonuclease G3BP assembles stress granules. J. Cell Biol. **160**:823–831.
37. **Wakita, T., et al.** 2005. Production of infectious hepatitis C virus in tissue culture from a cloned viral genome. Nat. Med. **11**:791–796.
38. **Weston, A., and J. Sommerville.** 2006. Xp54 and related (DDX6-like) RNA helicase: roles in messenger RNP assembly, translation regulation and RNA degradation. Nucleic Acids Res. **34**:3082–3094.
39. **White, J. P., A. M. Cardenas, W. E. Marissen, and R. E. Lloyd.** 2007. Inhibition of cytoplasmic mRNA stress granule formation by a viral proteinase. Cell Host Microbe **2**:295–305.
40. **Wilson, J. A., C. Zhang, A. Huys, and C. D. Richardson.** 2011. Human Ago2 is required for efficient miR-122 regulation of HCV RNA accumulation and translation. J. Virol. **85**:2342–2350.
41. **Yedavalli, V. S., C. Neuveut, Y. H. Chi, L. Kleiman, and K. T. Jeang.** 2004. Requirement of DDX3 DAED box RNA helicase for HIV-1 Rev-RRE export function. Cell **119**:381–392.
42. **Yi, Z., et al.** 2006. Subproteomic study of hepatitis C virus replicon reveals Ras-GTPase-activating protein binding protein 1 as potential HCV RC component. Biophys. Biochem. Res. Commun. **350**:174–178.
43. **You, L. R., et al.** 1999. Hepatitis C virus core protein interacts with cellular putative RNA helicase. J. Virol. **73**:2841–2853.
44. **Zufferey, R., D. Nagy, R. J. Mandel, L. Naldini, and D. Trono.** 1997. Multiply attenuated lentiviral vector achieves efficient gene delivery in vivo. Nat. Biotechnol. **15**:871–875.

Biochemical and Biophysical Research Communications 409 (2011) 663–668

Contents lists available at ScienceDirect

Biochemical and Biophysical Research Communications

journal homepage: www.elsevier.com/locate/ybbrc

Plural assay systems derived from different cell lines and hepatitis C virus strains are required for the objective evaluation of anti-hepatitis C virus reagents

Youki Ueda, Kyoko Mori, Yasuo Ariumi, Masanori Ikeda, Nobuyuki Kato *

Department of Tumor Virology, Okayama University Graduate School of Medicine, Dentistry, and Pharmaceutical Sciences, 2-5-1 Shikata-cho, Okayama 700-8558, Japan

ARTICLE INFO

Article history:
Received 8 April 2011
Available online 17 May 2011

Keywords:
HCV
HCV RNA replication system
Li23 cells
Reporter assay for anti-HCV reagents

ABSTRACT

Persistent hepatitis C virus (HCV) infection causes chronic liver diseases and is a global health problem. HuH-7 hepatoma-derived cells are widely used as the only cell-based HCV replication system for HCV research, including drug assays. Recently, using different hepatoma Li23-derived cells, we developed an HCV drug assay system (ORL8), in which the genome-length HCV RNA (O strain of genotype 1b) encoding renilla luciferase replicates efficiently. In this study, using the HuH-7-derived OR6 assay system that we developed previously and the ORL8 assay system, we evaluated 26 anti-HCV reagents, which other groups had reported as anti-HCV candidates using HuH-7-derived assay systems other than OR6. The results revealed that more than half of the reagents showed different anti-HCV activities from those in the previous studies, and that anti-HCV activities evaluated by the OR6 and ORL8 assays were also frequently different. In further evaluation using the HuH-7-derived AH1R assay system, which was developed using the AH1 strain of genotype 1b, several reagents showed different anti-HCV activities in comparison with those evaluated by the OR6 and ORL8 assays. These results suggest that the different activities of anti-HCV reagents are caused by the differences in cell lines or HCV strains used for the development of assay systems. Therefore, we conclude that plural HCV assay systems developed using different cell lines or HCV strains are required for the objective evaluation of anti-HCV reagents.

1. Introduction

Hepatitis C virus (HCV) infection frequently causes chronic hepatitis, which often leads to liver cirrhosis and hepatocellular carcinoma. Since approximately 170 million people are infected with HCV worldwide, HCV infection is a serious global health problem [1]. Although the combination of pegylated-interferon (PEG-IFN) and ribavirin is the standard therapy worldwide, only half of the patients receiving this treatment exhibit a sustained virologic response [2]. HCV is an enveloped virus with a positive single-stranded RNA virus of the *Flaviviridae* family. The HCV genome encodes a large polyprotein precursor of approximately 3000 amino acids, which is cleaved into 10 proteins in the following order: Core, envelope 1 (E1), E2, p7, non-structural 2 (NS2), NS3, NS4A, NS4B, NS5A, and NS5B [3,4].

To date, HuH-7 hepatoma-derived cells are used as the only cell culture system for robust HCV replication in HCV research, including drug assays. We have also developed a HuH-7-derived drug assay system (OR6), in which genome-length HCV RNA (O strain of genotype 1b derived from an HCV-positive blood donor) encoding renilla luciferase (RL) efficiently replicates [5]. Recently, we found a new human hepatoma cell line, Li23, that enables robust HCV RNA replication [6], and we showed that the gene expression profile of Li23 cells was distinct from that of HuH-7 cells, although both cell lines had similar liver-specific expression profiles [7]. In that study, we identified three genes (New York esophageal squamous cell carcinoma 1, β-defensin-1, and galectin-3) showing Li23-specific expression profiles by a comparative analysis using several other hepatic cell lines [7]. We further developed Li23-derived drug assay systems (ORL8 and ORL11), which are relevant to the HuH-7-derived OR6 assay system [6]. During the process of evaluating the ORL8 and ORL11 assay systems using anti-HCV reagents such as IFNs, we noticed that these assay systems were frequently more sensitive to anti-HCV reagents than the OR6 assay system [6]. Furthermore, we recently found that ribavirin at clinically achievable concentrations (approximately 10 μM) effectively inhibited HCV RNA replication in both the ORL8 and ORL11 assay systems, but not in the OR6 assay system [8]. This finding led to the clarification of the anti-HCV mechanism of ribavirin, and we demonstrated that ribavirin's anti-HCV activity was mediated by the inhibition of inosine monophosphate dehydrogenase, a key enzyme in the guanosine biosynthetic pathway [8]. From these findings, we supposed that the anti-HCV reagents reported to date might show different activities among the different drug assay systems. To test this assumption, we evaluated 22 anti-HCV reagents that were reported using HuH-7-derived assay systems other than OR6, using the OR6 and ORL8 assay systems. Four additional

* Corresponding author. Fax: +81 86 235 7392.
E-mail address: nkato@md.okayama-u.ac.jp (N. Kato).

0006-291X/$ - see front matter © 2011 Elsevier Inc. All rights reserved.
doi:10.1016/j.bbrc.2011.05.061

reagents predicted by antiviral activity other than HCV were also evaluated. Furthermore, a recently developed HuH-7-derived AH1R assay system (AH1 strain of genotype 1b derived from a patient with acute hepatitis) (Mori et al., in preparation) was also used for the evaluation. Here, we report that plural assay systems derived from different cell lines and different HCV strains are required for the objective evaluation of anti-HCV reagents.

2. Materials and methods

2.1. Cell cultures

HuH-7-derived OR6 and AH1R cells were maintained in medium containing G418 (0.3 mg/ml) as described previously [5]. Li23-derived ORL8 cells were also maintained in medium containing G418 (0.3 mg/ml) as described previously [6].

2.2. Reagents

Acetylsalicylic acid, cephalotaxine, clemizole, crucumin, isoliquiritigenin, nitazoxanide, and tizoxanide were purchased from Sigma–Aldrich (St. Louis, MO). Cantharidin, 2′-deoxy-5-fluorouridine, griseofulvin, guanazole, homoharringtonine, resveratrol, and Y7632 were purchased from WAKO Pure Chemical Industries, Ltd. (Osaka, Japan). Artemisinin and bisindoly maleimide 1 were purchased from Alexis Biochemicals (San Diego, CA). Artesunate and silibinin A were purchased from Lkt Laboratories (St. Paul, MN). Esomeprazole and nelfinavir were purchased from Toronto Research Chemicals (North York, ON, Canada). Cinanserin hydrochloride and HA1077 were purchased from Tocris Bioscience (Bristol, UK). 6-Azauridine was purchased from MP Biomedicals (Solon, OH). Carvedilol was purchased from Calbiochem (San Diego, CA). Hemin was purchased from Alfa Aesar (Ward Hill, MA). Methotrexate was purchased from Tokyo Chemical Industry (Tokyo, Japan). Cinanserin hydrochloride, guanazole, HA11077, and Y27632 were dissolved in the culture medium for Li23-derived cells. Artesunate was dissolved in 0.5% $NaHCO_3$ solution. Other reagents were dissolved in dimethyl sulfoxide.

2.3. RL assay

RL assay was performed as described previously [6]. Briefly, the cells were plated onto 24-well plates (2×10^4 cells per well) in triplicate and then treated with each reagent at several concentrations for 72 h. After treatment, the cells were subjected to luciferase assay using the RL assay system (Promega, Madison, WI). From the assay results, the 50% effective concentration (EC_{50}) of each reagent was determined.

2.4. WST-1 cell proliferation assay

The cells were plated onto 96-well plates (1×10^3 cells per well) in triplicate and then treated with each reagent at several concentrations for 72 h. After treatment, the cells were subjected to the WST-1 cell proliferation assay (Takara Bio, Otsu, Japan) according to the manufacturer's protocol. From the assay results, the 50% cytotoxic concentration (CC_{50}) of each reagent was determined.

2.5. Western blot analysis

The preparation of cell lysates, sodium dodecyl sulfate–polyacrylamide gel electrophoresis, and immunoblotting analysis were performed as previously described [9]. The antibodies used in this study were those against HCV Core (CP11; Institute of Immunology, Tokyo, Japan) and β-actin (AC-15, Sigma–Aldrich) as the control for the amount of protein loaded per lane. Immunocomplexes were detected with the Renaissance enhanced chemiluminescence assay (Perkin–Elmer Life Sciences, Boston, MA).

2.6. Selective index (SI)

The SI value of each reagent was determined by dividing the CC_{50} value by the EC_{50} value.

3. Results

3.1. Evaluation of 26 reagents for anti-HCV activity using OR6 and ORL8 assay systems

To obtain candidates for the evaluation of anti-HCV activity using OR6 and ORL8 assay systems, we first searched the literature in the PubMed database using the key words (HCV or hepatitis C) and (inhibit or antiviral or suppress or block); this yielded approximately 4500 reports published between January 2003 and April 2010. From these results, we further selected the reports in which the EC_{50} values of reagents were determined or estimated by the HuH-7-derived HCV assay systems using the Con-1 strain (genotype 1b) [10], N strain (genotype 1b) [11], or HCV JFH-1 strain (genotype 2a) [12]. We finally chose 22 commercially available reagents for the evaluation of anti-HCV activity using OR6 and ORL8 assay systems. Four reagents predicted from the antiviral activity (hepatitis B virus, cytomegalovirus, etc.) other than HCV were also included in the evaluation study. The 26 selected reagents and their references are listed in Supplementary Table S1.

For each of the 26 reagents, we determined the EC_{50} value by RL assay and the CC_{50} value by WST-1 assay using the OR6 or ORL8 assay system, and calculated the SI value by dividing the CC_{50} value by the EC_{50} value. For each reagent, we first compared the EC_{50} value obtained from the OR6 or ORL8 assay with that of the previous study. Consequently, we classified the 26 reagents into five classes, A to E (Table 1). Eight reagents (methotrexate, artemisinin, artesunate, clemizole, hemin, 6-azauridine, acetylsalicylic acid, and isoliquiritigenin with the order of the SI value in the ORL8 assay) belonged to class A, in which the EC_{50} value obtained by either the OR6 or ORL8 assay was less than one-third of that in the previous study (Supplementary Table S1 and Table 1). Artesunate, an artemisinin-derivative possessing antiviral activity against cytomegalovirus, herpesvirus, Epstein-Barr virus etc., was included in class A by the comparison with the data on anti-cytomegalovirus activity. In this class, we especially noticed that methotrexate (an anti-cancer drug) showed very strong anti-HCV activity (EC_{50} 0.1 μM; $CC_{50} > 200$ μM; SI > 2000) in the ORL8 assay (upper panel in Fig. 1A and Table 1), whereas methotrexate showed very weak anti-HCV activity ($EC_{50} > 200$ μM; $CC_{50} > 200$ μM) in the OR6 assay as well as in a previous report [13] (upper panel in Fig. 1A and Table 1). This drastic difference was confirmed by Western blot analysis (lower panels in Fig. 1A). These results indicate that only the ORL8 assay is drastically sensitive to methotrexate, and suggest that the anti-HCV activity of methotrexate depends on the types of hepatic cells. The comparison of the EC_{50} values of other reagents belonging to class A revealed that the ORL8 assay was more sensitive than the OR6 assay (1.9–15-fold) to artemisinin, artesunate, clemizole, acetylsalicylic acid, and 6-azauridine, and conversely the OR6 assay was more sensitive than the ORL8 assay (2–2.5-fold) to hemin and isoliquiritigenin (Table 1). Furthermore, the CC_{50} values of clemizole and 6-azauridine also differed more than twofold between the OR6 and OR8 assays (Table 1). These results suggest that the anti-HCV activities of these reagents are affected by the kind of assay systems used. Especially, we noticed that artemisinin and artesunate (antimalarial drugs) showed higher SI values in the

Table 1
Anti HCV activities of 26 reagents evaluated in this study.

	Assay	[a]		ORG		ORL8		AHIR	
	Cell origin	HuH-7		HuH-7		Li23		HuH-7	
	HCV strain	Con-1, N, JFH-1, etc.		O		O		AH1	
Class	Reagent	$\frac{CC_{50}}{EC_{50}}$	SI	$\frac{CC_{50}}{EC_{50}}$	SI	$\frac{CC_{50}}{EC_{50}}$	SI	$\frac{CC_{50}}{EC_{50}}$	SI
A	Methotrexate	$\frac{>100}{>100}$	–	$\frac{>200}{>200}$	–	$\frac{>200}{0.1}$	>2000	$\frac{170}{>200}$	<0.9
A	Artemisinin	$\frac{>177}{>78}$	>2.3	$\frac{380}{81}$	4.7	$\frac{370}{23}$	16	$\frac{310}{5.3}$	58
A	Artesunate[b]	$\frac{>15}{3.9}$	>3.8	$\frac{6.1}{2.3}$	2.7	$\frac{3.4}{0.22}$	15	$\frac{4}{0.81}$	4.9
A	Clemizole	$\frac{>20}{8}$	>2.5	$\frac{11}{22}$	0.5	$\frac{22}{2.0}$	11	$\frac{7.3}{>25}$	<0.3
A	Hemin	$\frac{>52}{22}$	>2.4	$\frac{10}{1.2}$	8.3	$\frac{18}{2.4}$	7.5	$\frac{7.2}{1.1}$	6.5
A	6-Azauridine	$\frac{>100}{100}$	>1.0	$\frac{10}{5.7}$	1.8	$\frac{1.5}{0.37}$	4.1	$\frac{14}{3.3}$	4.2
A	Acetylsalicylic acid	$\frac{8^{d}}{4^{d}}$	2.0	$\frac{2.6^{d}}{1.6^{d}}$	1.6	$\frac{2.4^{d}}{0.83^{d}}$	2.9	ND	–
A	Isoliquiritigenin	$\frac{<24}{24}$	<1.0	$\frac{12}{3.9}$	3.1	$\frac{15}{9.8}$	1.5	ND	–
B	Nelfinavir	$\frac{>10}{9.9}$	>1.0	$\frac{26}{11}$	2.4	$\frac{68}{12}$	5.7	ND	–
B	2′-Deoxy-5-fluorouridine	$\frac{<15}{15}$	<1.0	$\frac{31}{32}$	1.0	$\frac{36}{14}$	2.6	$\frac{13}{86}$	0.2
B	Resveratrol	$\frac{>10}{10}$	>1.0	$\frac{35}{4.3}$	8.1	$\frac{42}{16}$	2.6	$\frac{76}{9.9}$	7.7
B	Cantharidine[c]	$\frac{3.5}{0.3}$	12	$\frac{1.5}{0.28}$	5.4	$\frac{1.8}{0.69}$	2.6	ND	–
B	Homoharringtonine[c]	$\frac{0.5}{30^{e}}$	17	$\frac{38^{e}}{18^{e}}$	2.1	$\frac{0.11}{45^{e}}$	2.4	$\frac{22^{e}}{19^{e}}$	1.2
B	Crucumin	$\frac{>15}{15}$	>1.0	$\frac{18}{14}$	1.3	$\frac{19}{11}$	1.7	ND	–
B	Griseofulvin	$\frac{207}{6.1}$	34	$\frac{16}{4.4}$	3.6	$\frac{14}{8.6}$	1.6	ND	–
B	Cinanserin hydrochloride	$\frac{>10}{>10}$	–	$\frac{33}{25}$	1.3	$\frac{39}{35}$	1.1	ND	–
B	Cephalotaxine[c]	$\frac{>100}{60}$	>1.7	$\frac{35}{29}$	1.2	$\frac{38}{47}$	0.8	$\frac{4.8}{41}$	0.1
C	Tizoxanide	$\frac{15}{0.15}$	100	$\frac{11}{2.4}$	4.6	$\frac{24}{9.6}$	2.5	ND	–
C	Nitazoxanide	$\frac{38}{0.21}$	181	$\frac{11}{2.8}$	3.9	$\frac{17}{9.2}$	1.8	$\frac{7.2}{2.2}$	3.3
D	Guanazole	$\frac{<100}{>100}$	<1.0	$\frac{200}{>200}$	<1.0	$\frac{170}{>200}$	<0.9	$\frac{173}{>200}$	<0.9
D	HA1077	$\frac{50}{15}$	3.3	$\frac{>50}{>50}$	–	$\frac{>50}{>50}$	–	$\frac{>50}{>50}$	–
E	Bisindoly maleimide 1	$\frac{ND}{5}$	–	$\frac{8.1}{6.2}$	1.3	$\frac{15}{15}$	1.0	$\frac{14}{9.1}$	1.5
E	Esomeprazole	$\frac{ND}{>10}$	–	$\frac{67}{67}$	1.0	$\frac{27}{27}$	1.0	$\frac{20}{25}$	0.8
E	Y27632	$\frac{>50}{50}$	>1.0	$\frac{>80}{>80}$	–	$\frac{>80}{>80}$	–	$\frac{39}{>80}$	<0.5
E	Carvedilol	$\frac{17}{4.5}$	3.8	$\frac{4.4}{3.7}$	1.2	$\frac{6.6}{8.8}$	0.8	$\frac{6.3}{6.2}$	1.0
E	Silibinin A	$\frac{ND}{23}$	–	$\frac{12}{85}$	0.1	$\frac{26}{89}$	0.3	$\frac{28}{96}$	0.3

ND, not determined.
[a] Assay used in previous reports.
[b] Reported as anti-cytomegalovirus reagent.
[c] Reported as anti-hepatitis B virus reagent. EC_{50} and CC_{50} values are indicated by the order of μM except 'd' (μM) and 'e' (nM).

ORL8 assay than previously reported [14,15]. The anti-HCV profiles of artemisinin and artesunate in the OR6 and ORL8 assays are shown in Fig. 1B and Supplementary Fig. 1A, respectively. In addition, the comparison of SI values revealed that the OR6 assay was more sensitive to hemin and isoliquiritigenin than the HuH-7-derived assays (Con-1 and N strains) used in the previous reports (Supplementary Table S1), suggesting that the HCV strains used in the assay systems affect the evaluation of anti-HCV reagents.

Nine reagents (nelfinavir, 2′-deoxy-5-fluorouridine, resveratrol, cantharidin, homoharringtonine, crucumin, griseofulvin, cinanserin hydrochloride, and cephalotaxine with the order of SI value in the ORL8 assay) were placed in class B, in which the EC_{50} values obtained by the OR6 and ORL8 assays were similar (more than one-third to less than threefold) to those in the previous study (Table 1 and Supplementary Table S1). Cantharidin, homoharringtonine, and cephalotaxine, all of which possess anti-hepatitis B virus activity, were placed in class B by the comparison with the data on anti-hepatitis B virus activity (Supplementary Fig. 1).

Tizoxanide and nitazoxanide belonged to class C, in which the EC_{50} values obtained by both the OR6 and ORL8 assays were more than threefold higher than in the previous study (Table 1 and Supplementary Table S1). Guanazole and HA1077 were placed in class D, in which there was no anti-HCV activity in both the OR6 and ORL8 assays (Table 1). No anti-HCV activity of guanazole and HA1077 was also confirmed by Western blot analysis (data not shown). Lastly, five reagents (Bisindoly maleimide 1, esomeprazole, Y27632, carvedilol, and silibinin A) were placed in class E, in which pro-HCV activity was exhibited in both OR6 and ORL8 assays. We unexpectedly observed that these reagents enhanced the HCV RNA replication level. As a

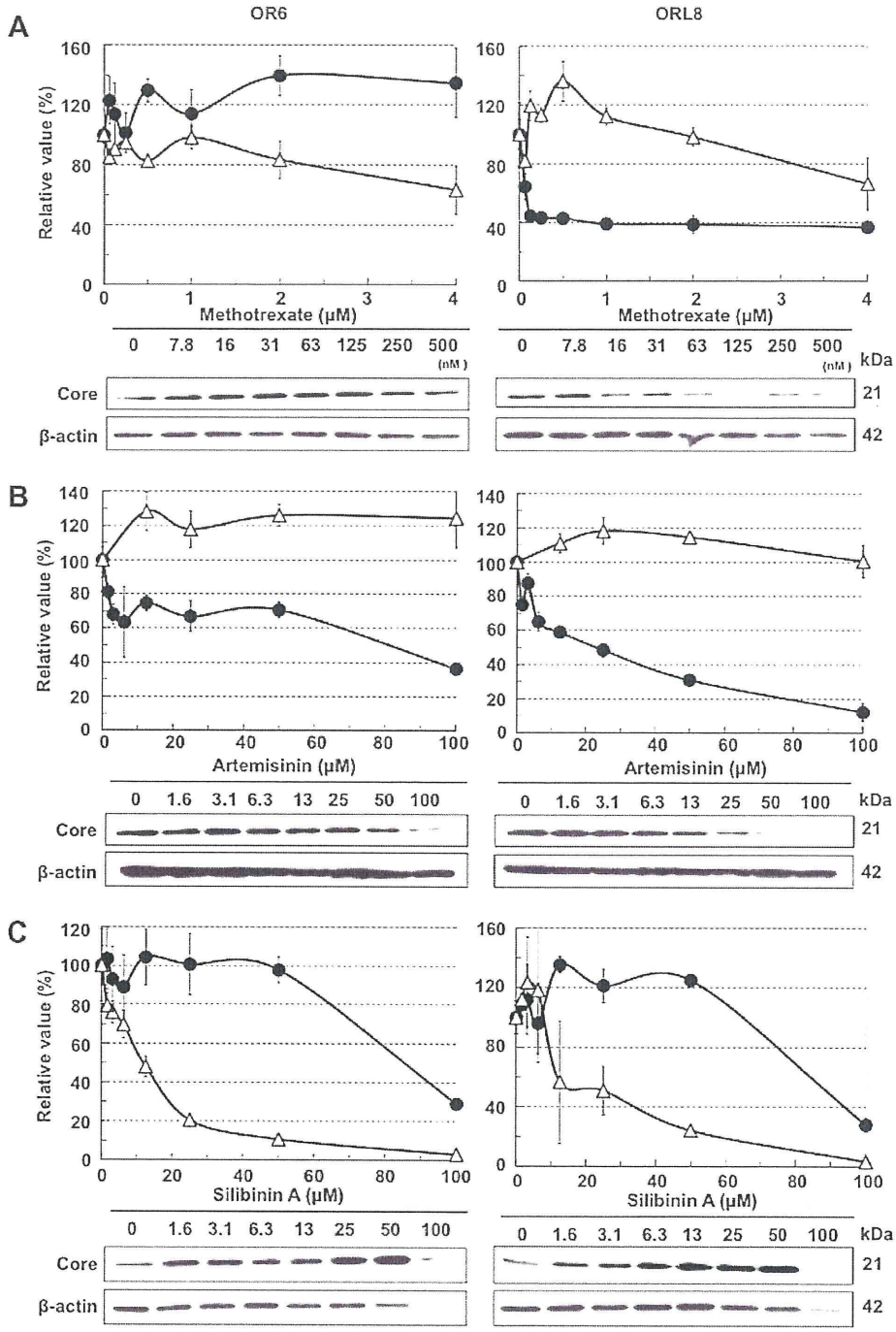

Fig. 1. Anti-HCV profiles of representative reagents in the OR6 and ORL8 assay systems. (A) Methotrexate sensitivities on genome-length HCV RNA replication in the OR6 and ORL8 assay systems. OR6 and ORL8 cells were treated with methotrexate for 72 h, followed by RL assay (black circle in the upper panel) and WST-1 assay (open triangle in the upper panel). The relative value (%) calculated at each point, when the level in nontreated cells was assigned to 100%, is presented here. Western blot analysis of the treated cells for the HCV Core was also performed (lower panel). (B) Artemisinin sensitivities on genome-length HCV RNA replication in the OR6 and ORL8 assay systems. RL assay, WST-1 assay, and Western blot analysis were performed as described in (A). (C) Silibinin A sensitivities on genome-length HCV RNA replication in the OR6 and ORL8 assay systems. RL assay, WST-1 assay, and Western blot analysis were performed as described in (A).

representative reagent, pro-HCV profiles of silibinin A are shown in the upper panel of Fig. 1C. These pro-HCV profiles were confirmed by Western blot analysis (lower panels in Fig. 1C for silibinin A and data not shown for the other reagents). Since the anti-HCV activity of silibinin A was detected by the HCV replicon assay system using the Con-1 strain [14], the converse effects obtained by our assay systems using the O strain may be due to the difference in HCV strains. In summary, the differences in anti-HCV activities observed among HuH-7- and Li23-derived assay systems used in this study and the other HuH-7-derived assay systems used in the previous studies suggest that the activities of anti-HCV reagents differ depending on which HCV strains and cell lines are used in the evaluation assays.

3.2. Evaluation of 18 reagents for anti-HCV activity using AH1R assay system

We previously established a HuH-7-derived cell line (AH1), which harbors genome-length HCV RNA (AH1 strain of genotype 1b) derived from a patient with acute hepatitis [16]. To further examine the effect of the HCV strain on anti-HCV reagent activity, we developed an AH1R assay system that is based on the AH1 cell line and that corresponds to the OR6 assay system (Mori et al., in preparation).

Using the AH1R assay system, we further evaluated the anti-HCV activities of 18 reagents, which showed differential anti-HCV activity between the OR6 and ORL8 assays, or showed either no anti-HCV activity or pro-HCV activity in both the OR6 and ORL8 assays. The results of the evaluation are shown in Table 1. The comparisons of the data obtained by the OR6 and AH1R assays revealed that the difference in the EC_{50} value from reagent to reagent was held within the range of one-third to threefold. However, we noticed that the EC_{50} value (5.3 μM) of artemisinin in the AH1R assay was remarkably lower than that (81 μM) in the OR6 assay (Supplementary Fig. 2 and Table 1), suggesting that artemisinin's anti-HCV activity differs depending on the HCV strain. Furthermore, the results of the AH1R assay revealed that cephalotaxine, belonging to class B, would be recategorized into class D. In summary, some reagents showed differential anti-HCV activities between the HuH-7-derived OR6 (O strain) and AH1R (AH1 strain) assay systems, although most of the reagents showed similar levels of anti-HCV activity in both assays. Taking together the results of the previous and present studies, we conclude that plural assay systems derived from different cell lines and HCV strains are needed for the objective evaluation of anti-HCV reagents.

4. Discussion

In the present study, we demonstrated for the first time that a Li23-cell-derived drug assay system, not a HuH-7-derived system, was important to use for the objective evaluation of anti-HCV reagents. In addition, we demonstrated that assay systems derived from different HCV strains were also necessary for the objective evaluation of anti-HCV reagents.

Among the 26 reagents evaluated by our assay systems, methotrexate showed the most drastic differences between the HuH-7- and Li23-derived assay systems in terms of anti-HCV activity. Although methotrexate showed very weak anti-HCV activity in the HuH-7-derived assay (Con-1 strain) used in a previous study [13] as well as in our OR6 and AH1R assays (O and AH1 strains), the ORL8 assay revealed very strong anti-HCV activity (SI > 2000). Such drastic differences in both assays suggest that some host factor or factors required for HCV RNA replication are different between these two cell lines, although the anti-HCV target of methotrexate is unclear. Since methotrexate is currently used as an anti-cancer drug or anti-rheumatic drug and its EC_{50} value for HCV RNA replication is 0.1 μM, it may be a potential candidate for enhancing the effects of the current combination therapy of PEG-IFN and ribavirin.

The anti-HCV activities of two antimalarial drugs, artemisinin and its derivative artesunate, are interesting. Although Paeshuyse et al. [14] showed that artemisinin possessed weak or moderate anti-HCV activity using a HuH-7- or HuH-6-derived subgenomic HCV replicon system, artemisinin's anti-HCV mechanism was unclear. On the other hand, Efferth et al. [15] reported that artesunate, the most studied artemisinin-derivative for the treatment of severe malaria, possessed antiviral activity against Epstein–Barr virus, human cytomegalovirus, human herpesvirus 6A, herpes simplex virus 1, and so on, except for HCV with the low micromolar range, although artesunate's precise antiviral mechanism was ambiguous. Therefore, we supposed, and our assay systems clearly detected, that both artemisinin and artesunate possess anti-HCV activity. Especially, the AH1R assay was the most sensitive to artemisinin (EC_{50} 5.3 μM), and the ORL8 assay was the most sensitive to artesunate (EC_{50} 0.22 μM). Preliminary experiments for the anti-HCV mechanisms of these reagents showed that they did not activate the IFN-signaling pathway (data not shown), and that they did not induce the oxidative stress (data not shown) as observed in the treatment with a broad range of anti-HCV reagents, including cyclosporine A [8,17]. Further studies are needed to clarify the anti-HCV mechanisms of these reagents. Since the largest SI value of artemisinin was 58 in the AH1R assay and that of artesunate was 16 in the ORL8 assay, these reagents may be also useful for the treatment of patients with chronic hepatitis.

In this study, we demonstrated that many anti-HCV reagents showed differential anti-HCV activities among different assay systems (OR6, ORL8, and AH1R) on HCV RNA replication. These results suggest that reliance on only a single assay system may lead to an incorrect evaluation of anti-HCV candidates. Therefore, we propose that plural assay systems derived from different cell lines and HCV strains should be used in order to evaluate anti-HCV candidates. Furthermore, plural assay systems derived from at least two different cell origins would be also useful for the screening of anti-HCV candidates.

Acknowledgments

We thank Yusuke Wataya and Hye-Sook Kim for their helpful discussions. This work was supported by grants-in-aid for research on hepatitis from the Ministry of Health, Labor, and Welfare of Japan. K. M. was supported by a Research Fellowship for Young Scientists from the Japan Society for the Promotion of Science.

Appendix A. Supplementary data

Supplementary data associated with this article can be found, in the online version, at doi:10.1016/j.bbrc.2011.05.061.

References

[1] D.L. Thomas, Hepatitis C epidemiology, Curr. Top. Microbiol. Immunol. 242 (2000) 25–41.
[2] S. Chevaliez, J.M. Pawlotsky, Interferon-based therapy of hepatitis C, Adv. Drug. Deliver. Rev. 59 (2007) 1222–1241.
[3] N. Kato, M. Hijikata, Y. Ootsuyama, et al., Molecular cloning of the human hepatitis C virus genome from Japanese patients with non-A, non-B hepatitis, P. Natl. Acad. Sci. USA 87 (1990) 9524–9528.
[4] N. Kato, Molecular virology of hepatitis C virus, Acta Med. Okayama 55 (2001) 133–159.
[5] M. Ikeda, K. Abe, H. Dansako, et al., Efficient replication of a full-length hepatitis C virus genome, strain O, in cell culture, and development of a luciferase reporter system, Biochem. Bioph. Res. Co. 329 (2005) 1350–1359.
[6] N. Kato, K. Mori, K. Abe, et al., Efficient replication systems for hepatitis C virus using a new human hepatoma cell line, Virus Res. 146 (2009) 41–50.
[7] K. Mori, M. Ikeda, Y. Ariumi, N. Kato, Gene expression profile of Li23 a new human hepatoma cell line that enables robust hepatitis C virus replication: comparison with HuH-7 and other hepatic cell lines, Hepatol. Res. 40 (2010) 1248–1253.
[8] K. Mori, M. Ikeda, Y. Ariumi, et al., Mechanism of action of ribavirin in a novel hepatitis C virus replication cell system, Virus Res. 157 (2011) 61–70.
[9] N. Kato, K. Sugiyama, K. Namba, et al., Establishment of a hepatitis C virus subgenomic replicon derived from human hepatocytes infected in vitro, Biochem. Bioph. Res. Co. 306 (2003) 756–766.
[10] V. Lohmann, F. Korner, J. Koch, et al., Replication of subgenomic hepatitis C virus RNAs in a hepatoma cell line, Science 285 (1999) 110–113.
[11] M. Ikeda, M. Yi, K. Li, S.M. Lemon, Selectable subgenomic and genome-length dicistronic RNAs derived from an infectious molecular clone of the HCV-N strain of hepatitis C virus replicate efficiently in cultured Huh7 cells, J. Virol. 76 (2002) 2997–3006.
[12] T. Wakita, T. Pietschmann, T. Kato, et al., Production of infectious hepatitis C virus in tissue culture from a cloned viral genome, Nat. Med. 11 (2005) 791–796.

[13] L.J. Stuyver, T.R. McBrayer, P.M. Tharnish, et al., Dynamics of subgenomic hepatitis C virus replicon RNA levels in Huh-7 cells after exposure to nucleoside antimetabolites, J. Virol. 77 (2003) 10689–10694.
[14] J. Paeshuyse, L. Coelmont, I. Vliegen, et al., Hemin potentiates the anti-hepatitis C virus activity of the antimalarial drug artemisinin, Biochem. Bioph. Res. Co. 348 (2006) 139–144.
[15] T. Efferth, M.R. Romero, D.G. Wolf, et al., The antiviral activities of artemisinin and artesunate, Clin. Infect. Dis. 47 (2008) 804–811.
[16] K. Mori, K. Abe, H. Dansako, et al., New efficient replication system with hepatitis C virus genome derived from a patient with acute hepatitis C, Biochem. Bioph. Res. Co. 371 (2008) 104–109.
[17] M. Yano, M. Ikeda, K. Abe, et al., Comprehensive analysis of the effects of ordinary nutrients on hepatitis C virus RNA replication in cell culture, Antimicrob. Agents Ch. 51 (2007) 2016–2027.

JMV-11-2638.R2(23250)

Journal of Medical Virology 9999:1–14 (2012)

Hepatitis C Virus Promotes Expression of the 3β-Hydroxysterol Δ24-Reductase Through Sp1

Makoto Saito,[1] Michinori Kohara,[2] and Kyoko Tsukiyama-Kohara[1]*

[1]*Department of Experimental Phylaxiology, Faculty of Life Sciences, Kumamoto University, Kumamoto, Japan*
[2]*Department of Microbiology and Cell Biology, Tokyo Metropolitan Institute of Medical Science, Tokyo, Japan*

Hepatitis C virus (HCV) establishes chronic infection, which often causes hepatocellular carcinoma. Overexpression of 3β-hydroxysterol Δ24-reductase (DHCR24) by HCV has been shown to impair the p53-mediated cellular response, resulting in tumorigenesis. In the present study, the molecular mechanism by which HCV promotes the expression of *DHCR24* was investigated. A significant increase in *DHCR24* mRNA transcription was observed in a cell line expressing complete HCV genome, whereas no significant difference in the expression of *DHCR24* was seen in cell lines expressing individual viral proteins. The 5′-flanking genomic region of *DHCR24* was characterized to explore the genomic region and host factor(s) involved in the transcriptional regulation of *DHCR24*. As a result, the HCV response element (−167/−140) was identified, which contains AP-2α, MZF-1, and Sp1 binding motifs. The binding affinity of the host factor to this response element was increased in nuclear extracts from cells infected with HCV and corresponded with augmented affinity of Sp1. Both mithramycin A (Sp1 inhibitor) and small interfering RNA targeting Sp1 prevented the binding of host factors to the response element. Silencing of Sp1 also downregulated the increased expression of *DHCR24*. The binding affinity of Sp1 to the response element was augmented by oxidative stress, whereas upregulation of *DHCR24* in cells expressing HCV was blocked significantly by a reactive oxygen species scavenger. Elevated phosphorylation of Sp1 in response to oxidative stress was mediated by the ATM kinase. Thus, activation of Sp1 by oxidative stress is involved in the promotion of expression of *DHCR24* by HCV. ***J. Med. Virol. 9999:1–14, 2012.*** © 2012 Wiley Periodicals, Inc.

KEY WORDS: HCV; DHCR24; Sp1; oxidative stress

INTRODUCTION

Hepatitis C virus (HCV) causes chronic hepatitis and hepatocellular carcinoma [Koike, 2007]. The estimated worldwide prevalence of HCV infection is 2.2–3.0% (130–170 million people) [Lavanchy, 2009], and chronic HCV infection is a major global public health concern. The most effective current treatment for HCV infection comprises combination therapy with PEGylated interferon-α and ribavirin [Bruchfeld et al., 2001; Lu et al., 2008]. However, this therapy has limited clinical efficacy, as sustained virological responses develop in only about half of patients infected with HCV genotype 1 [Kohara et al., 1995; Nakamura et al., 2002]. Efforts to develop therapies to treat HCV are also hindered by the high level of viral variation and the capacity of HCV to cause chronic infection. Therefore, there is an urgent need to develop effective treatments against chronic HCV infection.

Additional supporting information may be found in the online version of this article.

Grant sponsor: Ministry of Health and Welfare of Japan; Grant sponsor: Ministry of Education, Culture, Sports, Science and Technology of Japan; Grant sponsor: Program for Promotion of Fundamental Studies in Health Sciences of the National Institute of Biomedical Innovation; Grant sponsor: Cooperative Research Project on Clinical and Epidemiological Studies of Emerging and Re-emerging Infectious Diseases.

Kyoko Tsukiyama-Kohara present address is Transboundary Animal Diseases Center, Faculty of Agriculture, Kagoshima University, 1-21-24 Korimoto, Kagoshima-city 890-0065, Japan.

*Correspondence to: Kyoko Tsukiyama-Kohara, Department[Q1] of Experimental Phylaxiology, Faculty of Life Sciences, Kumamoto University, 1-1-1 Honjo, Kumamoto City, Kumamoto 860-8556, Japan. E-mail: kkohara@kumamoto-u.ac.jp, kkohara@agri.kagoshima-u.ac.jp

Accepted 16 January 2012

DOI 10.1002/jmv.23250
Published online in Wiley Online Library (wileyonlinelibrary.com).